JOURNAL OF GEOPHYSICAL RESEARCH, VOL. 112, D05206, doi:10.1029/2006JD007672, 2007

Refinements to the Köhler's theory of aerosol equilibrium radii, size spectra, and droplet activation: Effects of humidity and insoluble fraction

Vitaly I. Khvorostyanov[1] and Judith A. Curry[2]

Received 19 June 2006; revised 25 September 2006; accepted 18 October 2006; published 8 March 2007.

[1] Hygroscopic growth of mixed aerosol particles and activation of cloud condensation nuclei (CCN) are considered using Köhler theory without the assumption of a dilute solution and accounting for the effect of insoluble fraction. New analytical expressions are derived for the equilibrium wet radius of the wet aerosol and for the critical radii and supersaturations for CCN activation for both volume-distributed soluble fraction and a soluble shell on the surface of an insoluble core (e.g., mineral dust particle). These expressions generalize the known equations of the Köhler theory, and the accuracy and applicability of the classical expressions are clarified. On the basis of these new expressions, a general but simple method is derived for calculation of the wet size spectrum and the CCN activity spectrum from the dry aerosol size spectrum. The method is applicable for any arbitrary shape of the dry aerosol spectra. Some applications for evaluation of aerosol extinction and homogeneous ice nucleation in a polydisperse aerosol are briefly considered. The method described here can be used in cloud and climate models, in particular, for evaluation of the aerosol direct and indirect effects.

Citation: Khvorostyanov, V. I., and J. A. Curry (2007), Refinements to the Köhler's theory of aerosol equilibrium radii, size spectra, and droplet activation: Effects of humidity and insoluble fraction, *J. Geophys. Res.*, *112*, D05206, doi:10.1029/2006JD007672.

1. Introduction

[2] Interactions of atmospheric aerosol particles with humidity result in hygroscopic growth of aerosol particles and activation of the cloud condensation nuclei (CCN) into cloud drops. Hygroscopic growth influences aerosol radiative properties and the direct aerosol effect on climate; activation of cloud drops influences cloud microphysical and radiative properties and the first (albedo [*Twomey*, 1977]) and second (precipitation, [*Albrecht*, 1989]) indirect aerosol effects on climate. Both hygroscopic growth and CCN activation are described by the *Köhler* [1936] equation. The Kohler equation for the saturation ratio expresses the equilibrium size of the solution droplet as the balance between the curvature (Kelvin) effect and the solute (Raoult) effect.

[3] One of the major results of Köhler theory was the derivation of analytical expressions for the CCN critical radii r_{cr} and supersaturations s_{cr}. These quantities play a fundamental role in aerosol-cloud interactions since they determine the concentration of cloud drops, and have been widely used in cloud and climate studies for parameterizations of cloud drop formation (for overview references, see *Pruppacher and Klett* [1997] (hereinafter referred to as PK97) and *Seinfeld and Pandis* [1998]). The two key functions of drop activation are the differential, $\varphi_s(s_{cr})$, and integral or cumulative, $N_{CCN}(s_{cr})$, CCN activity spectra. The differential spectrum $\varphi_s(s_{cr})$ is an analog in the space of supersaturation of the CCN size spectrum in radius space, determines increase in activated CCN per a small increase of supersaturation and is a starting point for evaluation of cumulative spectrum $N_{CCN}(s_{cr})$ that determines the drop concentration formed at given s_{cr}. Knowledge of analytical expressions for r_{cr} and s_{cr} allow analytical evaluation of $\varphi_s(s_{cr})$ and $N_{CCN}(s_{cr})$ from the dry aerosol size spectrum $f_d(r_d)$. Such analytical expressions for r_{cr} and s_{cr} have been derived with $f_d(r_d)$ in the form of Junge-type power laws [e.g., *Levin and Sedunov*, 1966; *Sedunov*, 1974; *Fitzgerald*, 1975; *Smirnov*, 1978; *Khvorostyanov and Curry*, 1999a], and lognormal CCN size spectra [*von der Emde and Wacker*, 1993; *Ghan et al.*, 1993, 1995, 1997; *Feingold et al.*, 1994; *Abdul-Razzak et al.*, 1998; *Cohard et al.*, 1998, 2000; *Abdul-Razzak and Ghan*, 2000; *Nenes and Seinfeld*, 2003; *Rissman et al.*, 2004; *Fountoukis and Nenes*, 2005; *Khvorostyanov and Curry*, 2006].

[4] The hygroscopic growth of aerosol particles is usually characterized by the growth factor $GF(S_w) = r_w(S_w)/r_d$, where r_w and r_d are the wet and dry radii, and S_w is the water saturation ratio. The function $GF(S_w)$ and the humidity impact on aerosol extinction coefficient σ_{ext} are often parameterized with empirical relations of the type

$$GF(S_w) \sim (1 - S_w)^{-\alpha_1}, \tag{1a}$$

$$\sigma_{ext}(S_w) \sim (1 - S_w)^{-\alpha_2} \tag{1b}$$

[1]Central Aerological Observatory, Dolgoprudny, Russia.
[2]School of Earth and Atmospheric Sciences, Georgia Institute of Technology, Atlanta, Georgia, USA.

0148-0227/07/2006JD007672$09.00

where α_1 and α_2 are empirical parameters found by fitting experimental data [e.g., *Kasten*, 1969; *Hegg et al.*, 1996; *Kotchenruther et al.*, 1999; *Swietlicki et al.*, 1999; *Zhou et al.*, 2001] or by fitting functional dependencies for $GF(S_w)$ found from approximate analytical solutions of the Köhler equation [e.g., *Fitzgerald*, 1975; *Khvorostyanov and Curry*, 1999a, 1999b, 2006; *Swietlicki et al.*, 1999; *Cohard et al.*, 2000; *Kreidenweis et al.*, 2005; *Rissler et al.*, 2006]. A more detailed evaluation of $GF(S_w)$ is based on numerical solutions of the Köhler equation with comprehensive parameterizations of its parameters as functions of solution concentration [e.g., *Fitzgerald*, 1975; *Fitzgerald et al.*, 1982; *Hänel*, 1986; *Chen*, 1994; *Hämeri et al.*, 2000, 2001; *Brechtel and Kreidenweis*, 2000a, 2000b; *Snider et al.*, 2003]; this approach is used also to constrain aerosol physicochemical properties from the hygroscopic data for subsequent evaluation of r_{cr} and s_{cr}. The numerical solutions may be more precise and complete, but are more time consuming; the analytical dependencies are desirable since they provide a platform for development of simple and fast parameterizations for cloud and climate models.

[5] Analytical expressions for r_{cr} and s_{cr} have usually been determined from the Köhler equation with the following approximations: (1) high dilution in a haze drop, i.e., neglecting the insoluble CCN fraction in the denominator of Raoult's term, (2) soluble fraction proportional to the drop volume, and (3) small supersaturations. Concerns about each of these three assumptions are as follows.

[6] 1. Many recent field experiments have found aerosols with very small aerosol soluble fractions or aerosol particles that are nearly hydrophobic, often constituting a significant fraction of the total aerosol load. These field experiments have been conducted over many different regions: in desert areas [*Levin et al.*, 1996; *Rosenfeld et al.*, 2001; *Sassen et al.*, 2003]; the Arctic [*Leck et al.*, 2001; *Bigg and Leck*, 2001a, 2001b; *Curry et al.*, 2000; *Pinto et al.*, 2001]; and the Aerosol Characterization Experiments 1 and 2, ACE-1 and ACE-2 [*Swietlicki et al.*, 2000; *Snider et al.*, 2003]. Earlier detailed numerical calculations show that even at the time of activation, the degree of dilution (ratio of gained water mass to the dry mass) for the aerosol particles with small insoluble fraction $\sim$0.01 can be as low as 0.8 and $\sim$2 for the dry radii r_d = 0.02 and 0.1 μm, i.e., near the modal radii for many aerosols [e.g., *Hänel*, 1976; PK97, Table 6.3, p. 179]. Therefore the high dilution approximation may not be satisfied, and the mentioned observations indicate that analytical solutions to the Köhler equation without high dilution approximation are desirable.

[7] 2. The model of internally mixed aerosol particles with soluble fraction proportional to the particle volume has been challenged in several papers. A surface-proportional soluble shell was found in CCN measurements in several regions of eastern Europe [e.g., *Laktionov*, 1972; *Sedunov*, 1974]. *Levin et al.* [1996], *Falkovich et al.* [2001], and *Rosenfeld et al.* [2001] found that mineral dust particles coated with sulfate shells are typical in the eastern Mediterranean. It was hypothesized that several mechanisms may be responsible for such soluble shells, e.g., coagulation of the mineral dust with sulfate particles, deposition of sulfate on desert particles with oxidation of SO_2 or SO_4 on the particle surface, and nucleation of cloud drops on sulfate CCN with subsequent accumulation of mineral dust and evaporation of drops leaving sulfate coated dust. Simulations of heterogeneous chemical reactions and soluble shells on the dust surface showed their significant impact on the aerosol composition and on radiative forcing in the GISS GCM [*Wurzler et al.*, 2000; *Bauer and Koch*, 2005].

[8] 3. Some aerosol chambers reach very high supersaturations, $s \sim 15-25\%$, violating the assumption of small s. Since the lower limit of activated CCN is inversely proportional to s [*Sedunov*, 1974; *Ghan et al.*, 1993; *Khvorostyanov and Curry*, 1999a], this may lead to activation of very small aerosol particles with radii $r_d \ll 0.01$ μm, whose r_{cr} and s_{cr} can be different than those in the accumulation mode. Thus the approximation of small s should be eliminated for accurate interpretation of aerosol/cloud chamber experiments.

[9] The goals of this paper are to obtain approximate analytical solutions to the classical version of the Köhler equation that do not assume a highly dilute solution, volume proportional soluble fraction, or low supersaturation and to apply these expressions to the calculation of aerosol wet spectra and CCN activity spectra. In section 2, the equilibrium radii and growth factor of the deliquescent aerosol at subsaturation and in cloud are derived, and the accuracy of various approximations is estimated. Section 3 derives equations for the critical radii and supersaturations, and the accuracy of the classical expressions is briefly assessed. In sections 4 and 5 respectively, these expressions are used for derivation of the equilibrium wet aerosol size spectra and CCN activity spectra. Section 6 is devoted to a brief discussion of possible applications.

2. Equilibrium Radii and Size Spectra of Deliquescent Aerosol

[10] Subsequent to Köhler's pioneering work, based on the concept of Gibbs free energy, there have been numerous derivations of the Köhler equation from basic thermodynamical principles (balance of chemical potentials between the phases or entropy equation) with a variety of refinements [e.g., *Dufour and Defay*, 1963; *Defay et al.*, 1966; *Low*, 1969; *Mason*, 1971; *Sedunov*, 1974; *Young and Warren 1992*; PK97; *Chylek and Wong*, 1998]. Various modifications to Köhler theory accounted for the solubility limitation of the soluble CCN fraction which allowed description of deliquescence and humidity hysteresis [*Chen*, 1994]; absorption of the soluble gases by the haze drops that led to additional terms and yielded multimodal Köhler-type curves for CCN activation [*Kulmala et al.*, 1993; *Shulmann et al.*, 1996; *Laaksonen et al.*, 1998]; and finite time of dissolution of slightly soluble species that led to the smoothing of this multimodality [*Asa-Awuku and Nenes*, 2007]. A detailed analysis of various versions of the Köhler equation and of approximations in evaluation of its several basic parameters (solvent and solute volume additivity, surface tension, osmotic potential, and others) are given by *Brechtel and Kreidenweis* [2000a], *Charlson et al.* [2001], and *Kreidenweis et al.* [2005].

[11] In this work, we follow the approach developed by *Dufour and Defay* [1963] and PK97 and consider the "classical" version of the Köhler equation, which describes equilibrium water vapor pressure over a solution drop that

consists of highly soluble and insoluble components and is in equilibrium with ambient humid air.

2.1. Equilibrium Radii at Subsaturation

[12] The equilibrium radius of the wet aerosol $r_w(S_w)$ as a function of the ambient saturation ratio S_w and of the dry radius r_d can be obtained using the Köhler equation for S_w or supersaturation $s = (\rho_v - \rho_{vs})/\rho_{vs} = S_w - 1$ that can be written as [PK97]

$$\ln S_w = \frac{2\bar{v}_w \varsigma_{sa}}{RTr} - \frac{\nu\Phi_s \varepsilon_m M_w}{M_s \rho_w}\frac{m_d}{m_w}. \tag{2}$$

Here ρ_v, ρ_{vs} and ρ_w are the densities of vapor, saturated vapor and water, $\bar{v}_w \approx M_w/\rho_w$ is the molar volume of water in solution, M_w is the molecular weight of water, ζ_{sa} is the surface tension at the solution-air interface, R is the universal gas constant, T is the temperature (in degrees Kelvin), ν is the number of ions in solution, Φ_s is the osmotic potential, $\varepsilon_m = m_s/m_d$ is the mass soluble fraction, m_d is the mass of the dry aerosol particle, m_s and M_s are the mass and molecular weight of the soluble fraction, and m_w is the mass of water. The volume fraction ε_v is related to ε_m as $\varepsilon_v = \varepsilon_m(\rho_d/\rho_s)$, where ρ_d is the effective density of a dry aerosol particle, weighted by the densities of its soluble ρ_s and insoluble ρ_u fractions, $\rho_d = \varepsilon_v\rho_s + (1 - \varepsilon_v)\rho_u$. Using the simplifying assumptions on the constancy of the water molar volume in solution and the volume additivity of solvent (water) and solute (salt), $V = V_w + V_d$, which are good approximations for many common ionic solutes [*Dufour and Defay*, 1963; PK97; *Brechtel and Kreidenweis*, 2000a; *Kreidenweis et al.*, 2005], the ratio m_d/m_w can be expressed as $m_d/m_w = (\rho_d/\rho_w)[(r/r_d)^3 - 1]$. Substitution of these relations into (2) yields:

$$\ln S_w = \frac{A_k}{r} - \frac{B}{r^3 - r_d^3}. \tag{3}$$

$$A_k = \frac{2M_w\varsigma_{sa}}{RT\rho_w}, \qquad B = \frac{3\nu\Phi_s m_s M_w}{4\pi M_s \rho_w}. \tag{4}$$

Here A_k is the Kelvin curvature parameter, and the parameter B, called the activity of a nucleus, describes effects of the soluble fraction. Note that we do not assume $m_s \sim r_d^3$ in the numerator of the second term (4) as by PK97 and most other researchers.

[13] We employ a convenient parameterization of the soluble fraction and nucleus activity [*Levin and Sedunov*, 1966; *Sedunov*, 1974; *Smirnov*, 1978; *Khvorostyanov and Curry*, 1999a, 2006] that easily allows incorporation of alternative assumptions regarding the soluble fraction of the aerosol particle:

$$B = br_d^{2(1+\beta)} \tag{5}$$

where the parameters b and β depend on the chemical composition and physical properties of the soluble part of an aerosol particle. The parameter β describes the soluble fraction particle and decreases with increasing r_d since the solubility usually decreases with increasing particle size [e.g., *Sedunov*, 1974; PK97].

[14] For $\beta = 0.5$, the soluble fraction is proportional to the volume, $B \sim r_d^3$, and it was found in *Khvorostyanov and Curry* [1999a, 2006] that the quantity b is a dimensionless parameter:

$$b = (\nu\Phi_s)\varepsilon_v\frac{\rho_s}{\rho_w}\frac{M_w}{M_s} = (\nu\Phi_s)\varepsilon_m\frac{\rho_d}{\rho_w}\frac{M_w}{M_s}. \tag{6}$$

For $\beta = 0.5$, ε_v and ε_m do not depend on the dry radius r_d. The value of Φ_s, in general, also depends on r_w, however this effect on r_w, s_{cr} is weaker than those of the other factors [*Brechtel and Kreidenweis*, 2000a]. When evaluating b, Φ_s can be assigned some appropriate mean constant value (e.g., $\nu\Phi_s \approx 2.1$ for ammonium sulfate, rather than 3, which yields a good approximation [*Snider et al.*, 2003]), or the available parameterizations for Φ_s [e.g., *Brechtel and Kreidenweis*, 2000a] can be substituted into the final equations for r_w, r_{cr}, and s_{cr}. For example, using the typical parameters in (6) for the case $\beta = 0.5$ yields $b \approx 0.5$ for fully soluble nuclei ($\varepsilon_v = 1$), and $b \approx 0.25$ with $\varepsilon_v = 0.5$ for ammonium sulfate; $b \approx 1.33$ with $\varepsilon_v = 1$, and $b \approx 0.67$ with $\varepsilon_v = 0.5$ for NaCl.

[15] For $\beta = 0$, the activity $B = br_d^2$, i.e., mass m_s of soluble fraction is accumulated as a film or shell near the surface and is proportional to the surface area. The soluble volume fraction ε_v and b were parameterized by *Khvorostyanov and Curry* [1999a, 2006] as

$$\varepsilon_v = \varepsilon_{v0}\frac{r_{d,sc}}{r_d}, \qquad b = r_{d,sc}\varepsilon_{v0}(\nu\Phi_s)\frac{\rho_s}{\rho_w}\frac{M_w}{M_s}. \tag{7}$$

where $r_{d,sc}$ is some scaling radius and ε_{v0} is the reference soluble fraction (dimensionless). For this case, $b \sim r_{d,sc}$ and has the dimension of length. Such a model is based on the experimental data by *Laktionov* [1972], *Sedunov* [1974], *Levin et al.* [1996], *Falkovich et al.* [2001], *Rosenfeld et al.* [2001] and some theoretical models [*Wurzler et al.*, 2000; *Bauer and Koch*, 2005]. A detailed chemical analysis by *Levin et al.* [1996] showed that the surface density $P_s = m_s/S$ (S is the particle surface area) of the sulfates was fairly constant with particle size, $P_s \sim (2-6) \times 10^{-6}$ g cm^{-2}, in the range $r_d = 0.15$ to 10 μm. This indicates that $m_s \sim S \sim r_d^2$ and supports parameterization of soluble fraction mass proportional to the surface area with $\beta = 0$. Assuming a thin shell with the thickness $l_0 \ll r_d$, we can estimate l_0 from the relation $P_s = m_s/S \approx 4\pi\rho_s r_d^2 l_0/4\pi r_d^2 = l_0\rho_s$, or $l_0 = P_s/\rho_s$. With $\rho_s \sim 2$ g cm^{-2}, this yields an estimate $l_0 \sim 0.01-0.03$ μm, where $l_0 \ll r_d$ in this radii range. For this model of aerosol particles with a thin soluble shell, the soluble mass fraction is inversely proportional to the dry radius

$$\varepsilon_m = \frac{m_s}{m_d} \approx \frac{4\pi r_d^2 l_0 \rho_s}{(4/3)\pi r_d^3 \rho_d} = \frac{3l_0}{r_d}\frac{\rho_s}{\rho_d}, \tag{8}$$

Substituting this relation into (7), we obtain the parameter b that has the dimension of length [*Khvorostyanov and Curry*, 2006]

$$b = 3l_0(\nu\Phi_s)\frac{\rho_d}{\rho_w}\frac{M_w}{M_s}, \tag{9}$$

This parameterization requires knowledge of the soluble film thickness l_0 that can be obtained from experimental data [e.g., *Levin et al.*, 1996; *Falkovich et al.* 2001] or simulations [e.g., *Wurzler et al.*, 2000; *Bauer and Koch*, 2005].

[16] Note that the expressions in terms of the thin soluble film thickness are given for the illustrative purpose. If the soluble and insoluble masses are known, as in some current climate models, then the hygroscopicity can be expressed using parameterization (5), assuming the insoluble core geometry and proportionality of the soluble mass to the surface, i.e., $\beta = 0$. Then b can be determined and the equations given below applied.

[17] Using (5)–(9), Köhler's equation (3) can be rewritten as

$$\ln S_w = \frac{A_k}{r} - \frac{b r_d^{2(1+\beta)}}{r^3 - r_d^3}. \tag{10}$$

For dilute mixed haze particles, when $\ln S_w \approx s = S_w - 1$ and $r \gg r_d^3$, this equation is reduced to the commonly used dilute approximation

$$s = S_w - 1 = \frac{A_k}{r} - \frac{B}{r^3}. \tag{11}$$

[18] Various solutions for the humidity dependence of the wet particle radius $r_w(S_w)$ at subsaturation have been obtained in algebraic and trigonometric forms using *Kohler*'s equation (11) for dilute solutions or fully soluble particles [*Levin and Sedunov*, 1966; *Sedunov*, 1974; *Hänel*, 1976; *Fitzgerald*, 1975; *Fitzgerald et al.*, 1982; *Smirnov*, 1978; *Khvorostyanov and Curry*, 1999a, 2006; *Swietlicki et al.*, 1999; *Cohard et al.*, 2000; *Kreidenweis et al.*, 2005]. Here we generalize the expression of *Khvorostyanov and Curry* [1999a], and find analytical expressions for $r_w(S_w)$ without assuming a dilute solution and accounting for the insoluble fraction in the Raoult term, i.e., from (10). An approximate solution for $r_w(S_w)$ is given by *Khvorostyanov and Curry* [1999a].

[19] Finding a positive real root of the cubic equation (10) assuming $A_k = 0$, and then obtaining a correction due to A_k by expansion into the power series yields the following solution:

$$r_w(S_w) = r_d \left\{ 1 + \frac{b r_d^{2(1+\beta)-3}}{(-\ln S_w)} \left[1 + C(-\ln S_w)^{-2/3} \right]^{-3} \right\}^{1/3}, \tag{12}$$

$$C = \frac{A_k}{3 b^{1/3} r_d^{2(1+\beta)/3}}. \tag{13}$$

[20] Equation (12) can be simplified for a dilute wet particle, when (11) is applicable, allowing the neglect of the term 1 in the first bracket of (12):

$$r_{w1}(S_w) = \frac{b^{1/3} r_d^{2(1+\beta)/3}}{(1 - S_w)^{1/3}} \left[1 + C(1 - S_w)^{-2/3} \right]^{-1}. \tag{14}$$

This solution is valid under the condition of sufficiently large subsaturation $s < s_{lim}$, when the term with A_k is smaller than 1. An estimate from (14) with $b = 0.5$, $\beta = 0.5$, $A_k = 10^{-7}$ cm yields $s_{lim} = -0.8 \times 10^{-3}$ (-0.08%) for $r_d = 0.1$ μm and $s_{lim} = -2.4 \times 10^{-2}$ (-2.4%) for $r_d = 0.01$ μm. This is the upper limit for application of (12)–(14), hence these equations can be used up to $S_w \leq 0.95$–0.97 (relative humidity $H \leq 95$–97%) for the aerosol spectrum with $r_d \geq 0.01$ μm.

[21] The expression (14) was derived by *Khvorostyanov and Curry* [1999a] (a misprint in the index of r_w in that work is corrected here) assuming a dilute solution. It predicts humidity dependence $GF(S_w) \sim (1 - S_w)^{-1/3}$ for S_w lower than s_{lim}. The more general expression (12) predicts the same humidity dependence in the intermediate region of S_w, but weaker dependencies at lower values of $S_w < 0.7$–0.8 (in supersaturated solutions below deliquescence points in humidity hysteresis) and at higher values of $S_w > 0.9$. Similar functional forms were constructed by *Dick et al.* [2000], including the $(1 - S_w)^{-1/3}$ dependence but with additional polynomial terms containing 3 empirical parameters that were obtained by fitting experimental data on $GF(S_w)$. *Kreidenweis et al.* [2005] derived such dependencies from the Köhler equation by expanding the water activity into a power series and truncating after the first term; the resulting expressions also contained three fitting parameters. *Rissler et al.* [2006] used a similar expression, but reduced the number of empirical parameters to one. In contrast to these expressions with empirical parameters, (12) and (14) express $GF(S_w)$ directly in terms of the primary variables of the Köhler equation. The additional corrections due to dependencies on solution concentration of the surface tension ζ_{sa} (in A_k) and of the osmotic potential Φ_s (in b) can be introduced in (12)–(14) using the known parameterizations for these quantities [e.g., *Chen*, 1994; *Tang and Munkelwitz*, 1994; *Brechtel and Kreidenweis*, 2000a; *Hämeri et al.*, 2000, 2001].

[22] For particles with $r_d > 0.01$ μm and humidities lower than $S_w \sim 0.95$–0.97, the last term in the brackets in (12) can be neglected and the wet radius can be approximated as

$$r_{w2}(S_w) = r_d \left[1 + b r_d^{2(1+\beta)-3} (-\ln S_w)^{-1} \right]^{1/3}. \tag{15}$$

For dilute particles, we can neglect the first term in the bracket, then

$$r_{w3} = b^{1/3} r_d^{2(1+\beta)/3} (1 - S_w)^{-1/3}. \tag{16}$$

For $\beta = 0.5$, this equation reduces to $r_w = r_d \cdot b^{1/3} (1 - S_w)^{-1/3}$. This equation is similar to the empirical parameterization formulated by *Kasten* [1969] and the parameterization formulated from numerical calculations using Köhler's theory by *Fitzgerald* [1975]. Thus (16) provides a theoretical basis for the empirical dependencies for r_w and σ_{ext}, and (12)–(15) generalize them to account for the insoluble fraction in the wet aerosol.

[23] A comparison by *Khvorostyanov and Curry* [1999a] and here of (12)–(15) with the empirical parameterizations and calculations of $r_w(S_w)$ and $\sigma_{ext}(S_w)$ by *Kasten* [1969],

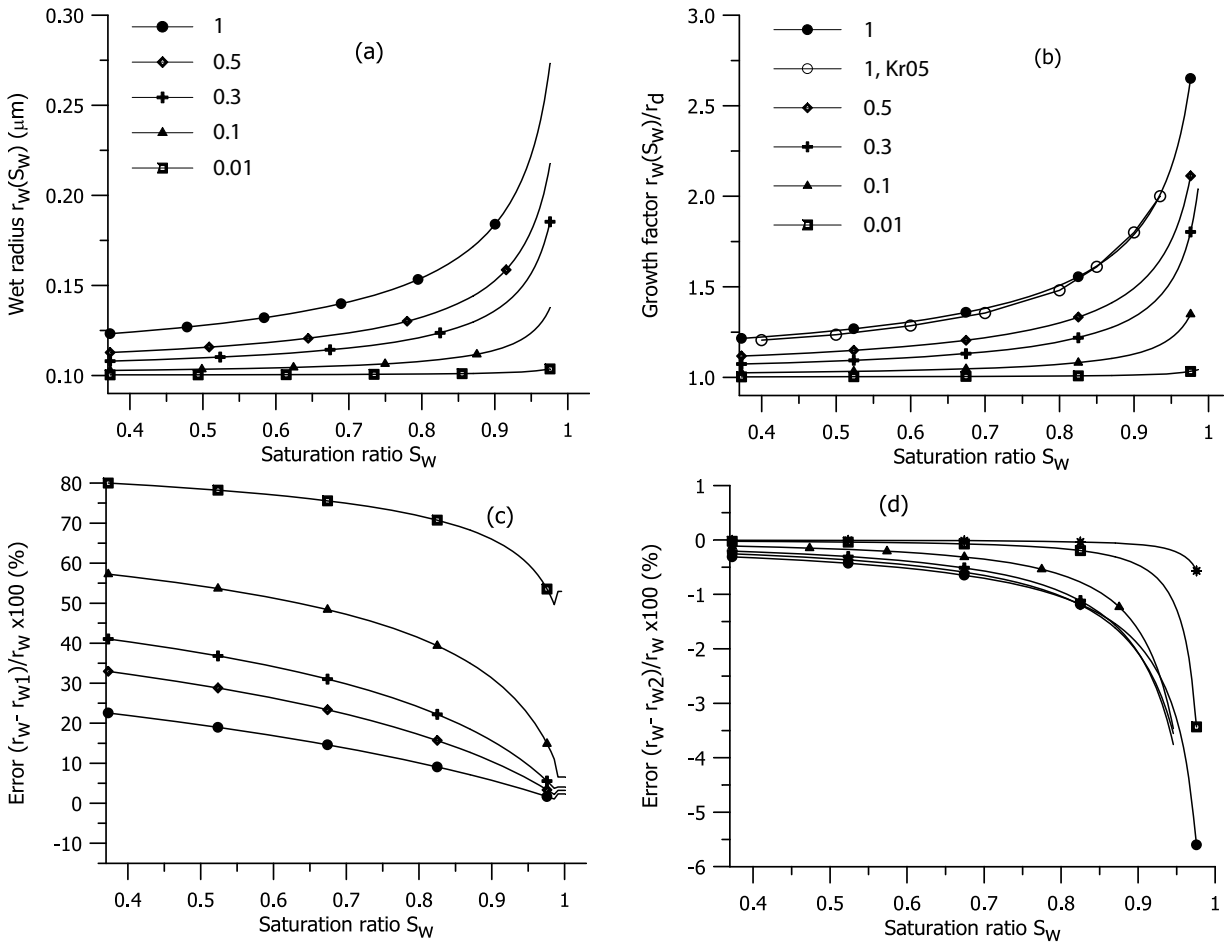

Figure 1. (a) Humidity dependence of the wet radii $r_w(S_w)$ calculated with (12) (solid circles), (b) growth factor r_w/r_d calculated with (12) (solid circles) in comparison with numerical calculations from *Kreidenweis et al.* [2005] (open circles), (c) the errors $\delta_1 = (r_w - r_{w1})/r_w \times 100$ with r_{w1} calculated from (14), and (d) $\delta_2 = (r_w - r_{w2})/r_w \times 100$ with r_{w2} calculated from (15). The values r_w, r_{w1}, and r_{w2} are calculated with $r_d = 0.1$ μm, $\beta = 0.5$, for various volume soluble fractions ε_v of ammonium sulfate indicated in the legend and b evaluated with (6).

Fitzgerald [1975], *Fitzgerald et al.* [1982], *Hänel* [1976], *Kotchenruther et al.* [2001], *Kreidenweis et al.* [2005] show that these equations still can be used as a reasonable approximation down to the lower humidities (30–40%) as can be reached by the deliquescent aerosol in the humidity hysteresis before spontaneous salt crystallization.

[24] Figures 1a and 1b show the humidity dependence of the wet radii $r_w(S_w)$ and the growth factor $r_w(S_w)/r_d$ calculated with the complete equation (12) for $\beta = 0.5$ and r_{w1}, r_{w2} calculated with approximate equations (14) and (15). A comparison of the calculated growth factor with precise numerical calculations from *Kreidenweis et al.* [2005] for pure ammonium sulfate particles (Figure 1b, solid and open circles) shows very good agreement and indicates a sufficiently high accuracy of (12). If the soluble fraction ε_v of ammonium sulfate is 0.3–1, r_{w1}, r_{w2}, and r_w/r_d increase by a factor of 2–3 in the region $0.3 < S_w < 1$ and increase especially rapidly at $S_w > 0.9$, in agreement with numerous experimental data and previous parameterizations cited above. This implies an increase of aerosol optical thickness by a factor of 4–9 and illustrates the strong humidity effect on aerosol radiative properties and direct aerosol effect on climate. The growth is much smaller for $\varepsilon_v = 0.1$, and is negligible for $\varepsilon_v = 0.01$. The error $\delta_1 = (r_w - r_{w1})/r_w \times 100$ in r_{w1} using the approximate equation (14) for dilute solutions increases with decreasing soluble fraction and reach 60–80% for $\varepsilon_v = 0.1$ to 0.01 (Figure 1c). The error of (15), $\delta_2 = (r_w - r_{w2})/r_w \times 100$, does not exceed 2–6% when $S_w < 0.97$ (Figure 1d). Thus (15), without assumption of a dilute solution, appears to be a much better approximation than (14), especially for evaluation of *GF* for less hygroscopic or nearly hydrophobic aerosol particles.

2.2. Equilibrium Radii of Interstitial Aerosol in a Cloud

[25] Equations (12)–(16) describe humidity transformations of the majority of wet CCN except for smallest particles at values of S_w approaching 1. At higher humidity within a cloud, $S_w \rightarrow 1$ ($s \rightarrow 0$), an alternative approximation should be used. By neglecting the insoluble fraction, the left hand side of (11) is zero, and the radius r_{wi}

Table 1. Transformation of Wet Radii r_w at High Saturation Ratios S_w for $\beta = 0.5$, $r_d = 0.1$ μm and Various Soluble Fractions ε_v and the Errors in Using Approximate Equations for r_w

	ε_v				
	1	0.5	0.3	0.1	0.01
$r_w(S_w = 0.98)$, μm	0.32	0.25	0.21	0.15	0.10
$r_w(S_w = 1.0)$, μm	0.69	0.49	0.39	0.23	0.14
$r_w(1.0)/r_w(0.98)$, μm	2.19	1.99	1.84	1.53	1.38
$\delta_2 = (r_w - r_{w2})/r_w \times 100$, % ($S_w = 0.98$)	1.05	2.18	3.72	10.9	49.6
$\delta_3 = (r_{wi} - r_{wi0})/r_{wi} \times 100$, % ($S_w = 1.0$)	2.31	3.20	4.04	6.55	52.9

of an interstitial wet aerosol particle can be found from the quadratic equation [e.g., *Curry and Webster*, 1999]:

$$r_{wi0}(S_w \cong 1) = \left(\frac{B}{A_k}\right)^{1/2} = r_d^{1+\beta}\left(\frac{b}{A_k}\right)^{1/2}, \qquad (17)$$

where the second equality is written with use of (5) for B and generalizes the known expression, $r_{wi0} \sim r_d^{3/2}$ with $\beta = 0.5$, for the other values of β; in particular, $r_{wi0} \sim r_d$ with $\beta = 0$. A generalization with account for the insoluble fraction can be done with the use of (10) at $S_w = 1$, which leads to a cubic equation

$$(r/r_d)^3 - \lambda(r/r_d) - 1 = 0, \qquad \lambda = br_d^{2\beta}/3A_k. \qquad (18)$$

The solution to (18) can be chosen in trigonometric or algebraic form, depending on the sign of $q = 1 - 4\lambda^3$. Trigonometric solution is convenient if $q < 0$, or $\lambda^3 > 1/4$, i.e., with sufficiently large soluble fraction. Then

$$r_{wi} = 2r_d^{1+\beta}\left(\frac{b}{3A_k}\right)^{1/2} \cos\left[\frac{1}{3}\arccos\left(\frac{3A_k}{4br_d^{2\beta}}\right)^{1/2}\right]. \qquad (19)$$

For an aerosol particle with $\beta = 0.5$ and $\varepsilon_m = 0.5$ of ammonium sulfate ($b = 0.25$), the condition $q < 0$ is equivalent to $r_d > 0.01$ μm, which is a typical case for many mixed CCN. For an aerosol particle with $\varepsilon_m = 10^{-2}$ and insoluble SiO_2 ($\rho_u = 2.65$ g cm^{-3}, $b = 8 \times 10^{-2}$), the condition $q < 0$ is equivalent to $r_d > 0.3$ μm, which is a typical case for dust particles with a thin soluble shell.

[26] The algebraic solution is more convenient if $q > 0$, or $\lambda^3 < 1/4$, i.e., for the small soluble fraction. Then

$$r_{wi} = \frac{r_d}{2^{1/3}}\left[\left(1 + q^{1/2}\right)^{1/3} + \left(1 - q^{1/2}\right)^{1/3}\right]. \qquad (20)$$

Note that (20) can be also used for $q < 0$, then $q^{1/2}$ is imaginary and the expressions $(1 \pm q^{1/2})$ become complex. However, the first and second brackets, $(1 \pm q^{1/2})^{1/3}$ are complex-conjugate and the entire expression is real.

[27] Consider the two limits that illustrate the particular cases with high and low soluble fractions.

[28] 1. The first limit is $\lambda = br_d^{2\beta}/3A_k \gg (1/4)^{1/3}$. Then in (19) for $b = 0.25$ and $r_d = 0.1$ μm, the argument of arccos is $\sim 0.036 \ll 1$, and arccos $\approx \pi/2$, thus the last term in (19) is $\approx \cos(\pi/6) = \sqrt{3}/2$, and (19) reduces to the classical case (17). A similar estimate is obtained from (20), expansion into a power series by λ^{-1} yields

$$r_{wi} \approx r_d\left(br_d^{2\beta}/3A_k\right)^{1/2}\left[i^{1/3} + \left(-i^{1/3}\right)\right], \qquad (21)$$

where $i = \sqrt{-1}$. Using the trigonometric Moivre's formula, one finds $\pm i^{1/3} = \cos(\pi/6) \pm i\sin(\pi/6) = \sqrt{3}/2 \pm i/2$, and the expression in the brackets is reduced to $\sqrt{3}$. Substitution into (21) yields $r_{wi} = r_d^{1+\beta}(b/A_k)^{1/2}$, i.e., (17). Thus (19) and (20) are generalizations of the classical equation (17) and reduce to it for the typical case with high soluble fractions.

[29] 2. The second limit is $\lambda = br_d^{2\beta}/3A_k \ll (1/4)^{1/3}$. Then expansion of (20) by λ gives

$$r_{wi} \approx r_d\left[1 + \frac{br_d^{2\beta}}{3A_k} - \frac{1}{3}\left(\frac{br_d^{2\beta}}{3A_k}\right)^3\right]. \qquad (22)$$

This case is relevant for particles of small sizes and small soluble fractions.

[30] Table 1 illustrates rapid increase of r_{wi} in the region $0.98 < S_w < 1$. Calculations are performed with (12) and (19) for the same parameters as in Figure 1, $\beta = 05$, $r_d = 0.1$ μm and various values of ε_v. For $\varepsilon_v = 1$ (fully soluble CCN), r_{wi} increases by a factor of 3 over the range $S_w = 0.3$ to 1, and increases by a factor of 2.2 over the range $S_w = 0.98$ to 1. The growth factors decrease with decreasing soluble fraction: for $\varepsilon_v = 0.01$, r_w increases by 0.4% only in the range $S_w = 0.3$ to 1 (Figure 1), and increases by 38% from $S_w = 0.98$ to 1 (Table 1). This rapid growth just below $S_w \to 1$ explains the sharp decrease in visibility and growth of aerosol optical thickness observed when aerosol transforms into "a milky haze" prior to activation (condensation) [e.g., *Kasten*, 1969; *Fitzgerald*, 1975].

[31] Table 1 shows calculations of the relative error of the classical equation (17), $\delta_3 = (r_{wi} - r_{wi0})/r_{wi} \times 100$, where r_{wi0} is calculated with (17), and r_{wi} with the new equation (19). The errors at $\varepsilon_v = 1$ are small (1–2%), and grow to 7–11% at $\varepsilon_v = 0.1$. For these values of ε_v, the accuracy of the classical equation (17) is acceptable. The errors grow to $\sim$50% at $\varepsilon_v = 0.01$; thus for very small ε_v, it is better to use the new equation (19). It is interesting to note that the relative error δ_2 defined in section 2.1 and δ_3 given in Table 1 are quite comparable, although are calculated with completely different equations. This indicates that the equations derived above describe $r_w(S_w)$ as a sufficiently smooth function at transition from subsaturation to interstitial conditions despite its rapid growth as $S_w \to 1$.

[32] The expressions (19) and (20) and the particular cases (21) and (22) are valid for S_w close to 1, and can be used at the stage of CCN activation or for interstitial unactivated cloud aerosol. In the latter case, $S_w > 1$ ($s > 0$), the spectra are limited by the boundary radius $r_b = 2A_k/3s$ [*Levin and Sedunov*, 1966; *Sedunov*, 1974; *Ghan et al.*, 1993; *Khvorostyanov and Curry*, 1999a, 2006].

3. Critical Radius and Supersaturation

[33] The expressions for the critical radius r_{cr} and supersaturation s_{cr} for CCN activation can be found using

Köhler's equation from the condition of the maximum, $ds/dr = 0$. For dilute solutions when $r_{cr} \gg r_d$, (11) yields a quadratic equation relative to r_{cr} with solutions [e.g., PK97; *Curry and Webster*, 1999]

$$r_{cr} = \left(\frac{3B}{A_k}\right)^{1/2} = r_d^{1+\beta}\left(\frac{3b}{A_k}\right)^{1/2}, \tag{23}$$

$$s_{cr} = \left(\frac{4A_k^3}{27B}\right)^{1/2} = \frac{2}{3}\frac{A_k}{r_{cr}} = r_d^{-(1+\beta)}\left(\frac{4A_k^3}{27b}\right)^{1/2}, \tag{24}$$

[34] The expressions on the right-hand side of (23), (24) are obtained using the parameterization of B in (5). However, if the soluble fraction is small (e.g., a thin soluble shell on the surface of an insoluble dust particle), the condition $r_{cr} \gg r_d$ can be invalid even at the time of activation, and the more complete equation (10) should be used instead of (11). To estimate the accuracy of (23) and (24), we obtain an analytical solution without the condition of high dilution at activation $r_{cr} \gg r_d$. The equation $ds(r_{cr})/dr_{cr}$ with $s_{cr}(r_{cr})$ defined by (10) yields a sixth-order equation in r_{cr}:

$$\frac{A_k}{r_{cr}^2} = \frac{3br_d^{2(1+\beta)}r_{cr}^2}{\left(r_{cr}^3 - r_d^3\right)^2}. \tag{25}$$

This can be reduced to the cubic equation by r_{cr},

$$r_{cr}^3 + ar_{cr}^2 - r_d^3 = 0, \qquad a = -\left(\frac{3b}{A_k}r_d^{2(1+\beta}\right)^{1/2}. \tag{26}$$

The solution to (26) is obtained as:

$$r_{cr} = r_d\chi(V), \qquad \chi(V) = [V + P_+(V) + P_-(V)], \tag{27}$$

$$P_\pm(V) = \left(V^3 \pm \left(V^3 + \frac{1}{4}\right)^{1/2} + \frac{1}{2}\right)^{1/3}, \qquad V = \left(\frac{br_d^{2\beta}}{3A_k}\right)^{1/2}. \tag{28}$$

Equation (27) is a generalization of (23) and reduces to it for the particular case $V \gg 1$. Then, expanding (27) and (28) into the power series yields

$$\begin{aligned} r_{cr} &\approx r_d\left[V + V\left(1 + \frac{V^{3/2}}{3}\right) + V\left(1 - \frac{V^{3/2}}{3}\right)\right] \\ &= 3r_dV = \left(\frac{3br_d^{2(1+\beta)}}{A_k}\right)^{1/2} = \left(\frac{3B}{A_k}\right)^{1/2}, \end{aligned} \tag{29}$$

which is the classical expression (23) for r_{cr}, confirming the validity of (27). In the opposite limit, $V \ll 1$, which may happen at very small soluble fractions or radii, another expansion of (27) by V yields

$$\begin{aligned} r_{cr} &\approx r_d\left(1 + V + \frac{2}{3}V^3\right) \\ &= r_d\left[1 + \left(\frac{br_d^{2\beta}}{3A_k}\right)^{1/2} + \frac{2}{3}\left(\frac{br_d^{2\beta}}{3A_k}\right)^{3/2}\right]. \end{aligned} \tag{30}$$

Using r_{cr} from (27), the critical supersaturation is then calculated from the equation

$$s_{cr} = \exp\left(\frac{A}{r_{cr}} - \frac{br_d^{2(1+\beta)}}{r_{cr}^3 - r_d^3}\right) - 1 = \exp\left(\frac{2A}{3r_{cr}}\right) - 1. \tag{31}$$

[35] Figures 2a and 2b depict the critical supersaturations, s_{cr}, and critical radii, r_{cr}, calculated with the new equations (31), (27) as functions of the dry radius r_d and volume soluble fraction ε_v from 1 to 10^{-3} for ammonium sulfate. Shown in Figures 2c and 2d are the relative errors in calculations of s_{cr} and r_{cr} defined as $\delta s_{cr} = (s_{cr,1} - s_{cr,2})/s_{cr,2}$, and $\delta r_{cr} = (r_{cr,2} - r_{cr,1})/r_{cr,2}$, where the index "1" denotes the classical expressions (23) and (24) and "2" denotes the new equations (31) and (27) that account for the insoluble fraction. The accuracy of the classical equations is reasonably good for the soluble fractions $\varepsilon_v \geq 0.1$ in accumulation (0.1–1 μm) and coarse (>1 μm) modes, the errors in s_{cr} and r_{cr} are smaller than 1–2%, (indicating also the correct limits of the new equations). For a particle of pure ammonium sulfate ($\varepsilon_v = 1$), the solution (31) exactly coincides with the precise numerical calculation from *Kreidenweis et al.* [2005]. The errors grow with decreasing r_d and ε_v. For $\varepsilon_v = 0.01$, the errors reach 15–25% in the accumulation mode. At $r_d = 0.01$ μm, they grow to 20–30% with $\varepsilon_v = 0.1$, and to 80–200% $\varepsilon_v = 0.01$. For the very small solubility of 10^{-3}, the errors are substantially greater, 100–500% for the submicron fraction 0.01–0.1 μm, and decrease to 1–20% for the coarse fraction.

[36] The accuracy and applicability of the classical expressions is further illustrated in Figure 3a, 3b, and 3c. The ratio r_{cr}/r_d decreases with decreasing solubility. For small $\varepsilon_v \sim 10^{-3}$ to 10^{-2}, the values of the critical and dry radii are comparable (lower curves in Figure 3a). The ratios r_{cr}/r_d evaluated with the new equation (27) for these small solubilities lie in accumulation mode slightly above the curve $r_{cr} = r_d$. So, $r_{cr}/r_d \sim 1$ and the relation $r_{cr} \gg r_d$, usually used in derivation of r_{cr} from (11) for dilute solutions, is not satisfied, hence (10), (25) and the solution (27) should be used instead under these conditions. Note that values $\varepsilon_v \sim 10^{-3}$ to 10^{-2} (the lower curves in Figure 3a) represents the case of mineral dust with thin soluble coating. The ratio r_{cr}/r_d calculated for these cases of small r_d and ε_v with the classical equation (23) lie below the curve $r_{cr} = r_d$ (Figure 3b), i.e., $r_{cr} < r_d$ and the classical expression fails as it predicts critical radii smaller that the dry ones. According to *Rosenfeld et al.* [2001], the fine-dispersed fractions of dust with small solubility may have a signif-

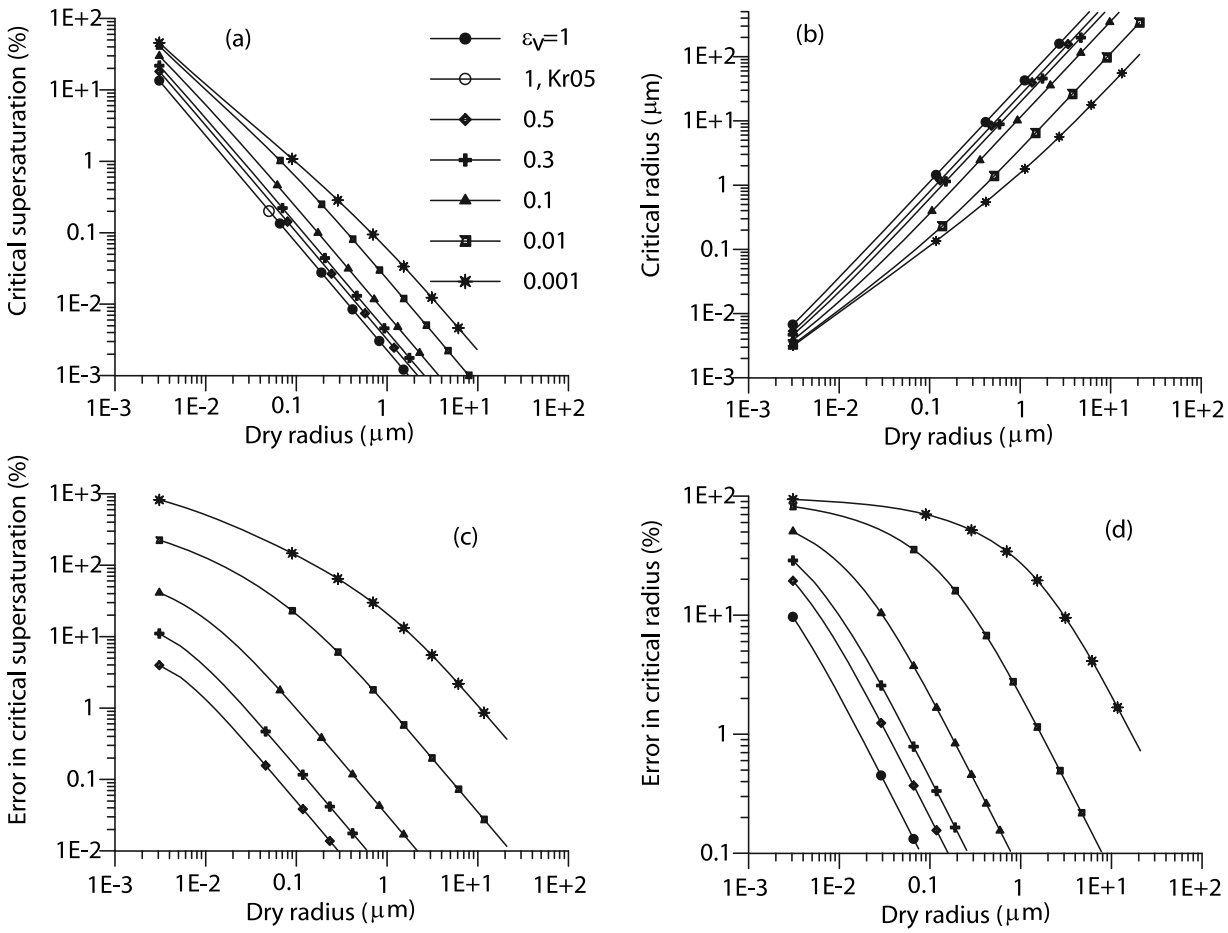

Figure 2. (a) Critical supersaturation s_{cr} (%) calculated with (31). The open circle is precise numerical calculation from *Kreidenweis et al.* [2005] for pure ammonium sulfate (ε_v = 1). (b) Radius r_{cr} (μm) calculated with (27). (c and d): Relative errors (%) of calculation with the old expressions (24) and (23) for s_{cr} and r_{cr} as functions of the dry radius and volume soluble fraction ε_v from 1 to 10^{-3} indicated in the legend.

icant climatic effect, since they may suppress precipitation in semiarid and arid areas and cause a desertification feedback loop. Hence its correct account in the models is important, and drop activation should be calculated with (27) and (31) rather than with (23) and (24).

[37] For $\varepsilon_v \geq 0.1$ and $r_d > 0.1$ μm, the ratio $r_{cr}/r_d \geq 4$, and the approximation $r_{cr}^3 \gg r_d^3$ with classical equations for r_{cr}, s_{cr} given by (23) and (24) becomes valid. Note that the 1000-fold decrease in the soluble fraction from 1 to 10^{-3} for r_d = 1 μm causes r_{cr} to decrease by only ~22 times from 37 μm to 1.6 μm, i.e., a mineral dust particle with thin soluble shell requires much less time for growth to activation size than a fully soluble CCN of same size. Figure 3c shows that $s_{cr,new}$ predicted by (31) for small $\varepsilon_v = 10^{-2}$ to 10^{-3} and small r_d is 3–9 times less than $s_{cr,old}$ predicted by the classical equation (24), which may substantially increase the activation process of such CCN.

[38] These estimates show that the classical expressions (23) and (24) should be used with caution for particles with small solubilities. A more precise approach for determining r_{cr} and s_{cr} is based on (27) and (31).

[39] The values of s_{cr} required for activation of a given CCN increase with decreasing r_d from 0.1–0.3% at r_d = 0.1 μm (a typical cloud case) to 2–12% at r_d = 0.01 μm and ε_v = 1 to 10^{-2} respectively and up to 10–50% at r_d = 0.003 μm. Thus s = 10–25%, as can be reached in a cloud chamber, may cause activation of accumulation and Aitken modes of CCN with r_d = 0.1 to 0.003 μm even with very small soluble fraction of 10^{-2}–10^{-3}. Hence analysis or numerical simulation of such cloud chamber experiments may require the more precise equations (27) and (31).

4. Size Spectra of Wet Aerosol

4.1. General Case of an Arbitrary Dry Spectrum

[40] We consider a polydisperse ensemble of mixed aerosol particles consisting of soluble and insoluble fractions that is described by the size spectrum of dry radii $f_d(r_d)$. As the saturation ratio S_w increases and exceeds the threshold of deliquescence $S_{w,del}$ of the soluble fraction, the hygroscopic growth of the particles begins and initially dry aerosol particles convert into wet "haze particles." The size

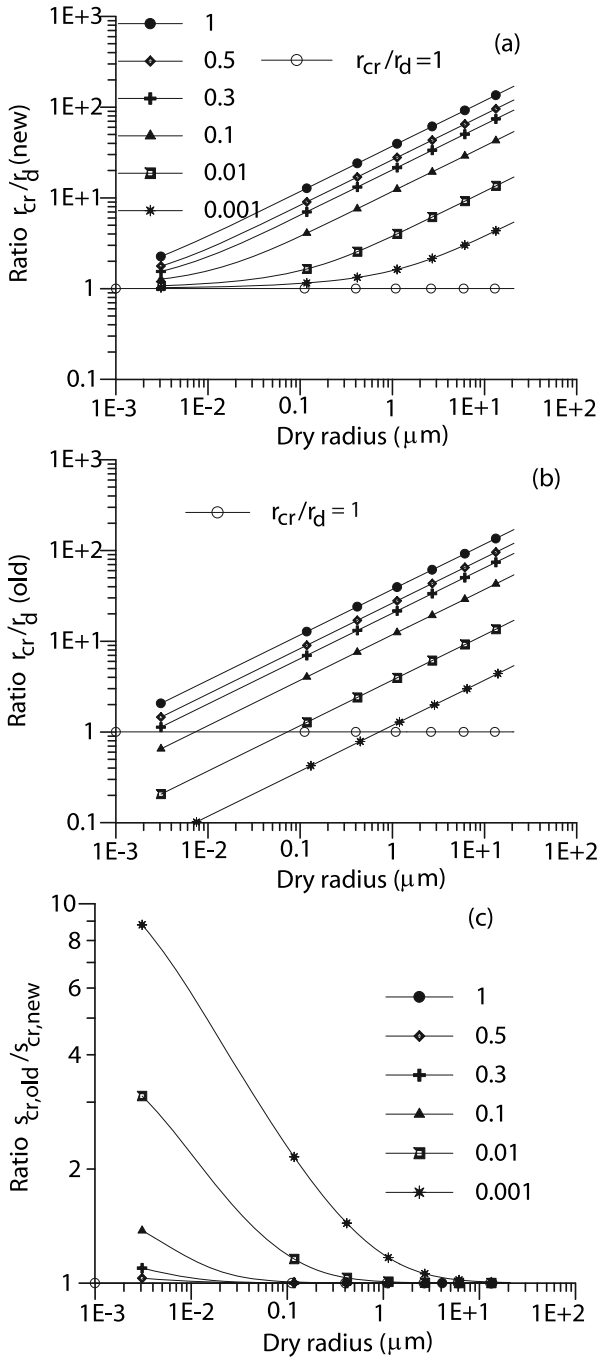

Figure 3. (a) Ratio of r_{cr}/r_d calculated with (27) (denoted "new"). (b) Same ratio calculated with (23) (denoted "old"). The dashed line with open circles is $r_{cr} = r_d$. (c) Ratio $s_{cr,old}/s_{cr,new}$ with $s_{cr,old}$ and $s_{cr,new}$ calculated with (24) and (31), respectively. The various soluble fractions ε_v are indicated in the legend.

spectrum of the wet aerosol $f_w(r_w)$ can be found from the differential conservation equation

$$f_w(r_w) = f_d[r_d(r_w)](dr_d/dr_w). \tag{32}$$

This equation requires knowledge of r_d as a function of r_w, which is the reverse problem relative to that considered in section 2 and again can be obtained from the cubic equation (10). For $\beta = 0.5$, we can solve (10) relative to r_d:

$$r_d(r_w) = r_w\varphi(r_w), \qquad \varphi(r_w) = \left[\frac{(-\ln S_w)r_w + A_k}{(-\ln S_w)r_w + A_k + br_w}\right]^{1/3}, \tag{33}$$

$$\frac{dr_d}{dr_w} = \varphi(r_w) - \frac{r_w\varphi^{-2}(r_w)}{3}\,\frac{A_k b}{[(-\ln S_w)r_w + A_k + br_w]^2}. \tag{34}$$

Substitution of (33) and (34) into (32) yields the wet spectrum $f_w(r_w)$.

[41] For the case $\beta = 0$, we obtain from (10) a cubic equation for $r_d(r_w)$ similar to (26) for r_{cr} in section 3, and the solution is

$$r_d = r_w\chi(r_w), \quad \chi(V_w) = V_w + P_+(V_w) + P_-(V_w), \tag{35}$$

$$\frac{dr_d}{dr_w} = \chi(V_w) + r_w\left\{\frac{dV_w}{dr_w} + V_w^2\left[P_+^{-2}(V_w)Q_+(V_w) + P_-^{-2}(V_w)Q_-(V_w)\right]\right\}, \tag{36}$$

where the functions $P_\pm(x)$ are defined in (28), and

$$Q_\pm(V_w) = \left(1 \pm \frac{1}{2}\left(V_w^3 + \frac{1}{4}\right)^{-1/2}\right), \tag{37}$$

$$V_w = \frac{b}{3[(-\ln S_w)r_w + A_k]}, \quad \frac{dV_w}{dr_w} = -\frac{b(-\ln S_w)}{3[(-\ln S_w)r_w + A_k)]^2}. \tag{38}$$

Substitution of (35)–(38) into (32) yields $f_w(r_w)$.

[42] The function $r_d(r_w)$ for the interstitial aerosol is obtained as the limit $-\ln S_w \approx 0$ in the above equation, which gives the smooth transition to size spectra of the wet interstitial aerosol.

[43] It should be emphasized that this method is not tied to any specific shape of the dry spectrum, but is suitable for any dry spectrum. This method can accommodate any analytical parameterization (e.g., Junge power law, lognormal, etc.) or a measured spectrum of any shape. Despite some algebraic complexity, these analytical equations are easy for coding and can be used for numerical calculation of the wet spectrum from the dry spectrum. The calculations of hygroscopic growth of the dry power law spectra [e.g., *Levin and Sedunov*, 1966; *Sedunov*, 1974; *Fitzgerald*, 1975; *Khvorostyanov and Curry*, 1999a; *Cohard et al.*, 2000], or lognormal spectra [e.g., *von der Emde and Wacker*, 1993; *Ghan et al.*, 1993; *Khvorostyanov and Curry*, 2006] or cross-sectional representation of the measured spectra [e.g., *Nenes and Seinfeld*, 2003] are particular cases of this approach.

4.2. Lognormal Dry Spectrum

[44] As discussed in section 2, for $\varepsilon_m \geq 0.1-0.2$, sufficient dilution and not very high humidity, $S_w < 0.95-0.97$, the terms with A_k can be neglected, and the relation between r_w and r_d can be described by (15) or (16), which can be written in the form

$$r_w = \alpha r_d^{\gamma}, \tag{39}$$

where α and γ are determined in (15), (16). The transformation to the wet spectra becomes especially simple if the size spectrum of dry aerosol $f_d(r_d)$ by the dry radii r_d can be represented by the lognormal distribution

$$f_d(r_d) = \frac{N_a}{\sqrt{2\pi}(\ln \sigma_d) r_d} \exp\left[-\frac{\ln^2 (r_d/r_{d0})}{2 \ln^2 \sigma_d}\right], \tag{40}$$

where N_a is the aerosol number concentration, σ_d is the dispersion of the dry spectrum and r_{d0} is the mean geometric radius related to the modal radius r_m as $r_m = r_{d0} \exp(-\ln^2 \sigma_d)$.

[45] For a lognormal spectrum, the transition to the wet spectra can be based on the simple rule by noting the following general and useful feature of the lognormal distributions. If we have a lognormal spectrum of radii r_d with the mean geometric radius r_{d0} and dispersion σ_d, then a nonlinear transformation of the variable of the form (39) that satisfies the conservation law (32) leads to the lognormal distribution again with the new parameters r_{w0}, and σ_w:

$$f_w(r_w) = \frac{N_a}{\sqrt{2\pi}(\ln \sigma_w) r_w} \exp\left[-\frac{\ln^2 (r_w/r_{w0})}{2 \ln^2 \sigma_w}\right]. \tag{41}$$

[46] The new mean geometric radius r_{w0} is related to r_{d0} according to the general transformation (39), and the wet dispersion is expressed via the dry one:

$$r_{w0} = \alpha r_{d0}^{\gamma}, \qquad \sigma_w = \sigma_d^{\gamma}. \tag{42}$$

This feature hereafter is referred to as "the first transformation property of the lognormal distribution" and is easily proven by substitution of (39), (40) into (32). We can use it to relate $f_d(r_d)$ and $f_w(r_w)$. For example, if the relation $r_w(r_d)$ for the wet aerosol with $\beta = 0.5$ at subsaturation is described by (15), it is a transformation (39) with

$$\gamma = 1, \qquad \alpha = \left[1 + b(-\ln S_w)^{-1}\right]^{1/3}. \tag{43}$$

In many cases for sufficiently dilute solutions, (16) is a good approximation as discussed in section 2, then $\gamma = 2(1 + \beta)/3$, $\alpha = b^{1/3}(1 - S_w)$. For the interstitial aerosol at $S_w \sim 1$, we find from the classical case (17), $\gamma = 1 + \beta$, and $\alpha = (b/A_k)^{1/2}$. Then, from the first transformation property of the lognormal distribution, we obtain that the dry spectrum (40) transforms into the wet spectrum (41), and its parameters r_{w0} and σ_w are related to the corresponding quantities r_{d0} and σ_d of the dry aerosol as:

$$r_{w0} = r_{d0}\left[1 + b(-\ln S_w)^{-1}\right]^{-1/3}, \quad \sigma_w = \sigma_d, \quad S_w < 0.97, \tag{44}$$

$$r_{w0} = r_{d0}^{2(1+\beta)/3} b^{1/3} (1 - S_w)^{-1/3}, \quad \sigma_w = \sigma_d^{2(1+\beta)/3}, \quad S_w < 0.97, \tag{45}$$

$$r_{w0} = r_{d0}^{(1+\beta)} (b/A_k)^{1/2}, \quad \sigma_w = \sigma_d^{(1+\beta)}, \quad S_w \cong 1. \tag{46}$$

Here, (44) corresponds to the $r_w(r_d)$ relation (15) with $\beta = 0.5$, and (45) to (16). The analytic form of the size spectrum (41) in these cases is the same at subsaturation and for the interstitial aerosol but the values of the mean geometric radius r_{w0} and dispersion σ_w are different as shown by (44)–(46). However, the transition from the subsaturation $S_w < 1$ to $S_w \sim 1$ is sufficiently smooth.

[47] The relations $r_w(r_d)$ of the form (39) have been suggested previously by *Levin and Sedunov* [1966], *Sedunov* [1974], *Fitzgerald* [1975], *Smirnov* [1978], *Khvorostyanov and Curry* [1999a, 2006] (see also this study, section 2), *Swietlicki et al.* [1999], *Kreidenweis et al.* [2005] as the parameterization of the calculations with Köhler theory, and by *Kasten* [1969], *Dick et al.* [2000], *Zhou et al.* [2001], *Rissler et al.* [2006] as fits to experimental data; each of these can be used for recalculation from the dry to the wet lognormal aerosol size spectrum using the first transformation property described above.

[48] The effect of humidity increase on the lognormal wet aerosol size spectra is shown in Figure 4. As predicted by (12) and (44), it results in gradual shift of the modal radius to larger values, with simultaneous decrease of the maxima. The transition to the limit $S_w = 1$ is fairly smooth, although there is a distinct decrease of the slopes. This resembles a corresponding effect for the power law spectra, when the transition to $S_w = 1$ is accompanied by a decrease of the Junge power index, e.g., $\mu = 4$ at $S_w < 1$ converts into $\mu = 3$ at $S_w \rightarrow 1$ over a very narrow humidity range [e.g., *Sedunov*, 1974; *Fitzgerald*, 1975; *Smirnov*, 1978; *Khvorostyanov and Curry*, 1999a].

[49] The simplified equations (39)–(46) can be used in many cases for not very low dilutions and soluble fractions, while the more complete equations (32)–(38) can be used otherwise. The application of any of these methods depends on the specific aerosol spectra, and the choice of the method can be justified for a given situation under consideration.

4.3. Inverse Power Law Spectrum

[50] The aerosol size spectra are often represented as the Junge-type inverse power laws:

$$f_{d,w}(r_{d,w}) = c_{d,w} r^{-\mu_{d,w}}, \tag{47a}$$

$$c_{d,w} = N_a(\mu - 1) r_{\min}^{\mu-1} \left[1 - (r_{\min}/r_{\max})^{\mu-1}\right], \tag{47b}$$

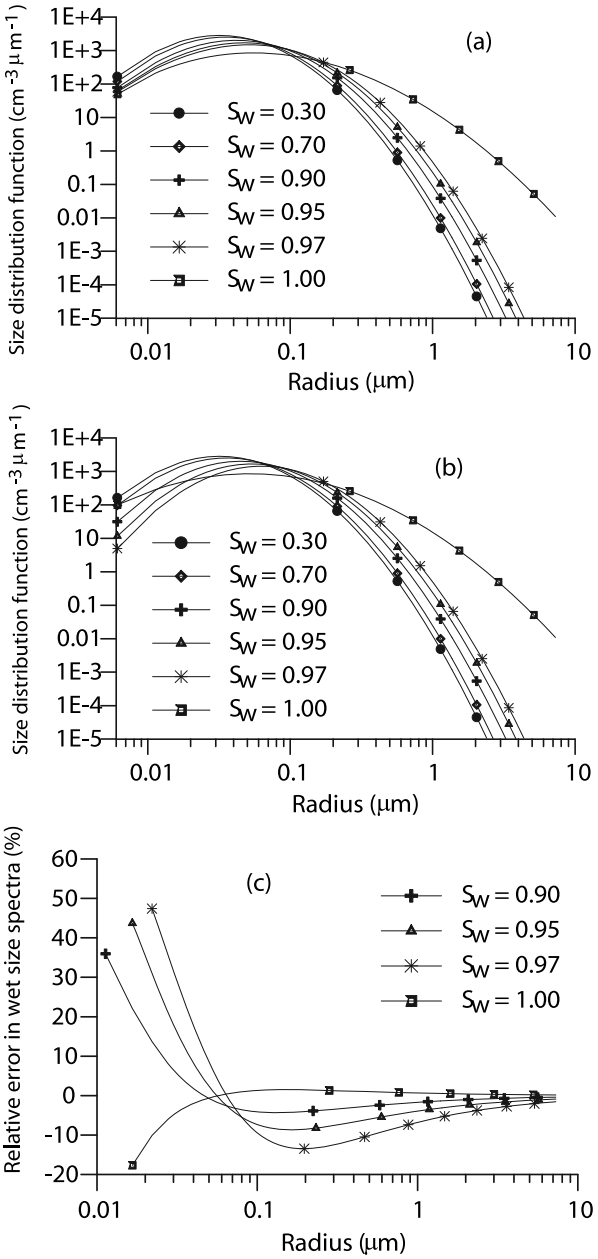

Figure 4. Humidity dependence of the wet aerosol size spectra. (a) Full spectra $f_{w1}(r_w)$ calculated with (32)–(34) and complete equation (12) for $r_w(S_w)$. (b) Approximate spectra $f_{w2}(r_w)$ calculated with transformation (42) and (43) using shortened equation (15) for r_w. (c) Relative error $\delta_{fw} = (f_{w1} - f_{w2})/f_{w1} \times 100$ (%). Calculations are made for the initial lognormal dry spectrum ($r_{d0} = 0.03$ μm, $\sigma_d = 2.0$), $\beta = 0.5$, $b = 0.25$ (50% of ammonium sulfate), and several S_w indicated in the legend. In case $S_w > 1$ ($s > 0$) the spectra should be limited by the boundary radius $r_b = 2A/3s$.

where μ is the power index, $c_{d,w}$ is the normalizing factor, the spectrum is normalized to aerosol concentration N_a by integration from $r_{\min}$ to $r_{\max}$, and the indices "d, w" mean dry or wet aerosol. The second term in the brackets in (47b) can be usually neglected since $r_{\min} \ll r_{\max}$. Consider the case with $\beta = 0.5$. If $S_w < 0.97$ and $r_d \geq 0.01$ μm, then (33) and (34) can be simplified by neglecting A_k in φ and in the denominator of dr_d/dr_w. Substituting (47a), (47b) for the dry aerosol into (32), and using (33) and (34) with these simplifications, we obtain after some transformations:

$$f_w(r_w) = c_d \varphi^{-(\mu-1)} \left[1 - \frac{bA_k}{3r_w(-\ln S_w)^2}\varphi^3\right] \approx N_a(\mu-1) r_{\min}^{\mu-1} r_w^{-\mu} \left(1 + \frac{b}{-\ln S_w}\right)^{(\mu-1)/3} \cdot \left[1 - \frac{bA_k}{3r_w(-\ln S_w)^2}\left(1 + \frac{b}{-\ln S_w}\right)\right] \quad (47c)$$

Hence the dry power law spectrum (47a) with the index $-\mu$ transforms at subsaturation into the wet spectrum, which is a superposition of the two power laws with the indices $-\mu$ and $-(\mu + 1)$; the second of these becomes significant at $S_w \geq 0.95$. The wet power law spectra were derived by *Levin and Sedunov* [1966], *Fitzgerald* [1975], *Smirnov* [1978], [*Khvorostyanov and Curry*, 1999a] for sufficiently diluted solutions. Equation (47c) is a generalization of these works that allows using this spectrum down to substantially smaller humidities. Besides the parameter b, the impact of insoluble fraction is described by the first term 1 in the rounded parentheses, and lower humidities are more accurately represented using $-\ln S_w$ instead of $(1 - S_w)$ as in the previous works. If $b/(-\ln S_w) \gg 1$, then 1 can be neglected in the rounded parentheses; if also $-\ln S_w \approx (1 - S_w)$, then (47c) is reduced to the expressions derived by *Khvorostyanov and Curry* [1999a]. Equation (47c) is used in section 1 to illustrate humidity and wavelength dependencies of aerosol extinction coefficients.

[51] Both lognormal and power laws have their own advantages and deficiencies and were used for analysis or simulation of various aerosol properties, usually as independent tools, although in many cases the correspondence between them is desirable. A link between the Junge and lognormal spectra was found in *Khvorostyanov and Curry* [2006], where it was shown that the lognormal spectra (40), (41) can be presented at every point by a power law (47a) with the indices μ and normalizing factors $c_{d,w}$ being the functions of the corresponding radii $r_{d,w}$:

$$\mu_{d,w}(r_{d,w}) = 1 + \frac{\ln(r_{d,w}/r_{d0,w0})}{\ln^2 \sigma_{d,w}}, \quad (48)$$

$$c_{d,w}(r_{d,w}) = f_{d,w}(r_{d,w}) r_{d,w}^{\mu}, \quad (49)$$

where r_{d0}, r_{w0} are the mean geometric radii, σ_d, σ_w are the dispersions; those for the wet aerosol are defined by (44)–(46).

[52] The properties of these effective power law indices for a dry aerosol were considered by *Khvorostyanov and Curry* [2006], and Figure 5 shows the indices of the wet aerosol. The indices are negative at smaller r (corresponding to the growing branch on the left from the modal radius of lognormal spectra) and become positive at larger r (to the right of the mode of lognormal spectrum). An increase in S_w at $S_w < 1$ results in the parallel shift of the curves, since the

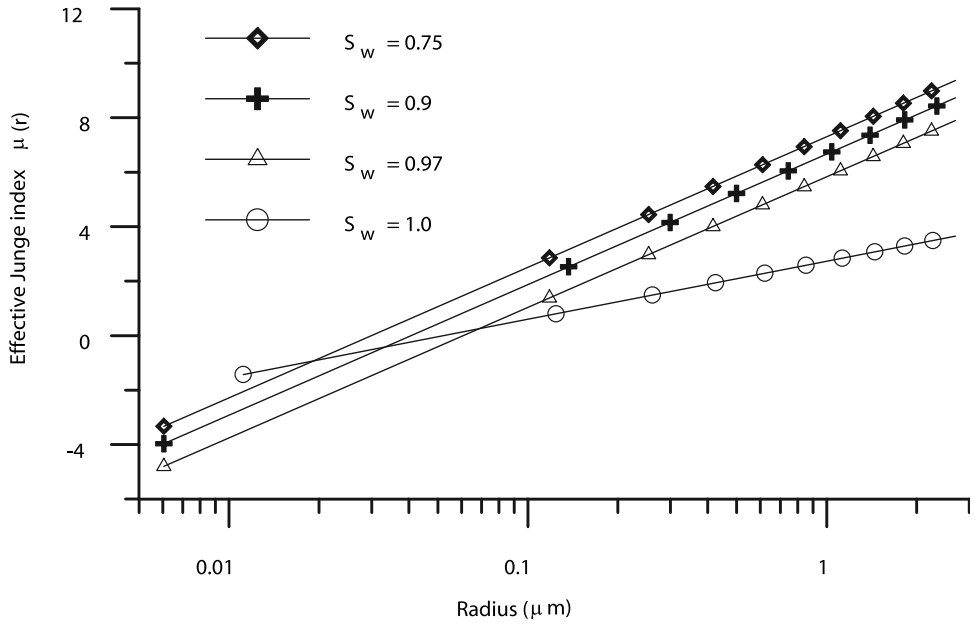

Figure 5. Dependence on the saturation ratio S_w of the power indices $\mu(S_w)$ of the wet aerosol approximating the lognormal distributions calculated from (48) and r_{w0}, σ_w calculated from (44) and (46). The parameters of the dry aerosol are modal radius $r_m = 0.03$ μm, dispersion $\sigma_d = 2$, $\beta = 0.5$, and $b = 0.25$.

increasing humidity causes the growth of the mean radius but the dispersion does not depend on S_w and does not change at $S_w < 1$ (see (44) and (45)). When $S_w \approx 1$, the μ indices decrease similarly to the power laws for dry aerosol.

5. Modification of CCN Activation Power Law

5.1. General Case of an Arbitrary Dry Spectrum

[53] The CCN differential supersaturation activity spectrum $\varphi_s(s_{cr})$ can be obtained from the size spectrum of the dry CCN similar to the wet spectra in section 4 using the conservation law in differential form:

$$\varphi_s(s_{cr}) = -f_d[(r_d(s_{cr})](dr_d/ds_{cr}). \tag{50}$$

Here s_{cr} is the critical supersaturation required to activate a dry particle with radius r_d; the minus sign occurs since increase in $dr_d > 0$ corresponds to a decrease in $ds_{cr} < 0$. To use (50), we need to know r_d as a function of s_{cr} or of r_{cr}, since the relation of s_{cr} and r_{cr} is given by (31). This is a reverse problem relative to that considered in section 3 and again can be obtained from (25), which reduces now to

$$r_d^3 + a_{cr} r_d^{2(1+\beta)} - r_{cr}^3 = 0, \quad a_{cr} = \frac{b r_{cr}}{A_k - r_{cr}\ln(1+s_{cr})}. \tag{51}$$

For $\beta = 0.5$, we obtain a solution for $r_d(s_{cr})$ from (51) and using the relation $r_{cr} = (2/3)A_k/\ln(1 + s_{cr})$ that follows from (31):

$$r_d(s_{cr}) = \frac{2A_k}{3\ln(1+s_{cr})}\xi(s_{cr}), \quad \xi(r_{cr}) = \left[1 + \frac{2b}{\ln(1+s_{cr})}\right]^{-1/3}. \tag{52}$$

The function dr_d/ds_{cr}, required for (50) can be calculated from (52)

$$\frac{dr_d}{ds_{cr}} = -\frac{2A_k\xi(s_{cr})}{3(1+s_{cr})\ln^2(1+s_{cr})}\left[1 - \frac{2b}{3[2b + \ln(1+s_{cr})]}\right]. \tag{53}$$

[54] Now, the differential activity spectrum $\varphi_s(s_{cr})$ (50) can be calculated using (52) and (53) for any shape of the dry size spectrum $f_d(r_d)$ for $\beta = 0.5$.

[55] For a CCN with $r_d \gg 0.01$ μm and not very small soluble fraction, then $s_{cr} \ll b$, and $\ln(1 + s_{cr}) \approx s_{cr}$, and approximately

$$\xi(s_{cr}) \approx (1 + 2b/s_{cr})^{-1/3} \approx (s_{cr}/2b)^{1/3}. \tag{54}$$

Substituting this into (52), we obtain

$$r_d(s_{cr}) = \left(4A_k^3/27b\right)^{1/3} s_{cr}^{-2/3} \tag{55}$$

[56] Inverting (55) for $s_{cr}(r_d)$, we obtain (24), and hence (52) is an inversion of the $s_{cr} - r_d$ relation (27). For this limiting case, we obtain from (53):

$$dr_d/ds_{cr} = -(4A_k/9)(2b)^{-1/3} s_{cr}^{-5/3}, \tag{56}$$

which can be obtained directly from (55) and verifies the validity of (53).

[57] For the case $\beta = 0$, (51) becomes a cubic equation similar to (26) but with unknown r_d, and it is useful to choose

a solution depending on the sign of $y = 1/4 - (b/A_k)^3$. If $y < 0$, or $b/A_k > (1/4)^{1/3}$, then it is convenient to select a trigonometric solution

$$r_d(s_{cr}) = \frac{2b}{3\ln(1+s_{cr})}\psi(U), \quad U = \frac{b}{A_k}, \tag{57}$$

$$\psi(U) = 2\cos\left[\frac{1}{3}\arccos\left(\frac{1}{2U^3} - 1\right)\right] - 1, \tag{58}$$

$$\frac{dr_d}{ds_{cr}} = -\frac{r_d(s_{cr})}{(1+s_{cr})\ln(1+s_{cr})}. \tag{59}$$

[58] If $y > 0$, or $b/A_k < (1/4)^{1/3}$, then a convenient solution is algebraic

$$r_d(s_{cr}) = r_{cr}\chi(V_{cr}), \quad \chi(V) = [V_{cr} + P_+(V_{cr}) + P_-(V_{cr})],$$
$$V_{cr} = -U = -b/A_k, \tag{60}$$

and the functions $P_\pm(z)$ are defined in (28). This solution could be used also for $b/A_k > (1/4)^{1/3}$. The definition (28) for $P_\pm(z)$ shows that $P_\pm(z)$ become then complex, but $P_+(z)$ and $P_-(z)$ are complex-conjugate and the solution is real. The function dr_d/ds_{cr} is expressed for this case also by (59).

5.2. Lognormal Dry Spectrum

[59] For a lognormal spectrum $f_d(r_d)$ with the mean geometric radius r_{d0} and dispersion σ_d, a nonlinear transformation of the variable of the form

$$s_{cr} = \alpha r_d^{-\gamma}, \tag{61}$$

satisfies the relation (50) and gives again the lognormal distribution by the variable s_{cr} with the new parameters s_0, and σ_s. The new mean geometric radius is then related to r_{d0} according to the general transformation (61), and the new dispersion is expressed via the old one:

$$s_0 = \alpha r_{d0}^{-\gamma}, \quad \sigma_s = \sigma_d^{\gamma}. \tag{62}$$

This feature is hereafter referred to as "the 2nd transformation property of lognormal distributions," can be proved by substitution of (61) into (50), and is similar to the 1st transformation property in section 4, except for the different powers of s_0, σ_s. It follows from (24) that for dilute solutions, when $r_{cr} \gg r_d$,

$$\alpha = \left(\frac{4A_K^3}{27b}\right)^{1/2}, \quad \gamma = 1 + \beta. \tag{63}$$

Using the 2nd transformation property, we find that the dry lognormal CCN size spectrum (40) by r_d corresponds to the lognormal CCN activity spectrum $\varphi_s(s_{cr})$ by s_{cr} of the same form (40) but with the mean geometric supersaturation s_0 instead of r_{d0} and dispersion σ_s instead of σ_d:

$$s_0 = \left(\frac{4A_k^3}{27b}\right)^{1/2} r_{d0}^{-(1+\beta)}, \quad \sigma_s = \sigma_d^{(1+\beta)}. \tag{64}$$

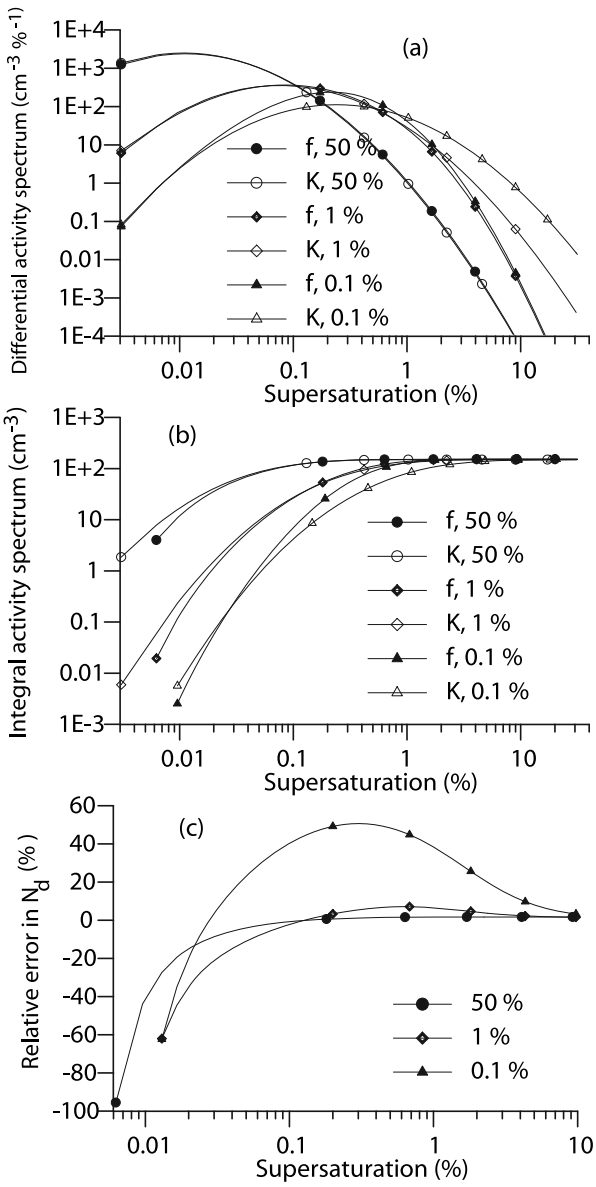

Figure 6. (a) Differential activity spectra $\varphi_s(s_{cr})$, (b) integral activity spectra $N_{CCN}(s_{cr})$, and (c) relative error defined in the text, calculated with the two methods: (1) for the dry lognormal size spectrum (40) with the full equations (50)–(53) (symbol *f*, solid symbols) and (2) as the lognormal distribution for $\varphi_s(s_{cr})$ with s_0 and σ_s based on the approximation of the classical Köhler theory (64) (symbol *K*, open symbols). Calculations are performed with $\beta = 0.5$, $N_d = 150$ cm^{-3}, $r_m = 0.03$ μm, and $\sigma_d = 2.15$. The numbers near the curves indicate volume soluble fraction of ammonium sulfate in percent.

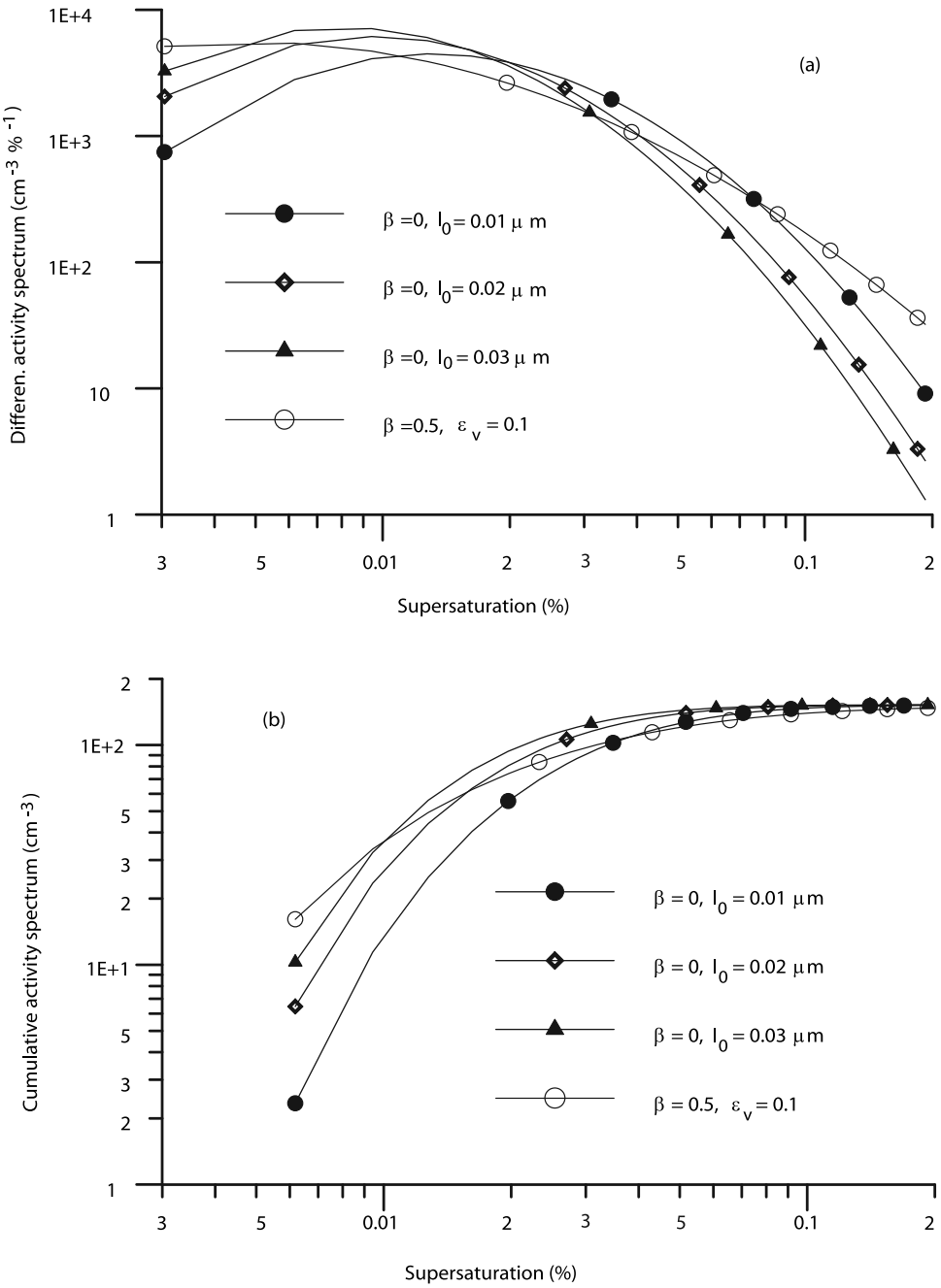

Figure 7. (a) Differential and (b) cumulative CCN activity spectra calculated with $\beta = 0$, equations (50) and (57)–(60), and various thicknesses l_0 of the soluble film on the surface of an insoluble core and compared with the case $\beta = 0.5$ with soluble fraction $\varepsilon_v = 0.1$. The dry size spectra are lognormal with $r_m = 0.3$ μm and $\sigma_d = 2.15$.

The equations for transition from the dry CCN size spectra to the differential activity spectra were obtained by *von der Emde and Wacker* [1993], *Ghan et al.* [1993], *Abdul-Razzak et al.* [1998], *Fountoukis and Nenes* [2005] for $\beta = 0.5$ and were generalized by *Khvorostyanov and Curry* [2006] for the other values of β. Using the 2nd transformation property makes the transition from the dry size spectra to the activity spectra automatic and very simple once we define the $s_{cr} - r_d$ relation (e.g., (61)).

[60] Figure 6 shows a comparison of the differential activity spectra $\varphi_s(s_{cr})$, integral activity spectra $N_{CCN}(s_{cr})$ and relative error $\delta_{NCCN} = (N_{CCN}(f) - N_{CCN}(K))/N_{CCN}(f) \times 100$, calculated with the two different methods: (1) using the dry lognormal size spectrum (40) and the full equations (50)–(53) (symbol f) and (2) as the lognormal distribution for $\varphi_s(s_{cr})$ with s_0 and σ_s based on the approximation of the classical Köhler theory (64) (symbol K). Calculations are performed with $\beta = 0.5$, $N_d = 150$ cm^{-3}, $r_m = 0.03$ μm, $\sigma_d = 2.15$ and various volume soluble fractions of ammonium sulfate in percent. Although the approximate classical method overestimates $N_{CCN}(s)$ by 10–40% at $s < 0.02$, the general agreement of both methods is good enough for

$\varepsilon_v > 10^{-2}$. For smaller ε_v, the classical approximation underestimates $N_{CCN}(s)$ by 40–55% in the region $s = 0.1$–0.6%, where the major activation process occurs. Thus the new more complete equations (50)–(53) predict much more rapid activation at small soluble fractions than the approximate method.

[61] Shown in Figure 7 are the differential and cumulative CCN activity spectra calculated for $\beta = 0$ with (50) and (57)–(60) for CCN with the soluble film of thickness l_0 on the surface of an insoluble core. The dry size spectra are chosen as a model of the coarse mode, lognormal with $r_m = 0.3$ μm and $\sigma_d = 2.15$. The values of b are calculated with (9) and l_0 estimated from the data of *Levin et al.* [1996] as described in section 2.1. The results for $\beta = 0$ are compared with the case $\beta = 0.5$, $\varepsilon_v = 0.1$ and the same dry spectrum. Figure 7 shows that N_{CCN} with $\beta = 0$ and thicknesses $l_0 = 0.03$, 0.02 and 0.01 μm becomes greater than that with $\beta = 0.5$ at s > 0.01, 0.015 and 0.04% respectively, although in the latter two cases the soluble fractions in CCN with $\beta = 0$ is substantially smaller. This example shows that CCN such as dust particles coated with soluble films can be more effective than CCN with soluble fractions homogeneously distributed in volume, suggesting an important role of mineral dust in cloud nucleation.

6. Applications of the Wet Aerosol Size Spectra

6.1. Aerosol Optics

[62] The aerosol extinction coefficient σ_λ^{ext} is given by the formula:

$$\sigma_\lambda^{ext}(S_w) = \pi \int_{r_{\min}}^{r_{mzx}} r_w^2 f_w(r_w) Q_{ext}(x, n_w) dr_w, \qquad (65)$$

where $Q_{ext}(x, n_w)$ is the extinction efficiency, λ is the wavelength, $x = 2\pi r_w/\lambda$ is the size parameter, n_w is the aerosol refractive index, and $r_{\min}$ and $r_{\max}$ are limits of integration. Substituting the wet lognormal spectrum from (41) with the wet parameters from (45), (46) into (65), we obtain

$$\sigma_\lambda^{ext}(S_w) = D_{1,ext}(S_w)(1 - S_w)^{-2/3} I_{ext}(S_w), \quad S_w < 1, \qquad (66)$$

$$D_{1,ext}(S_w) = \frac{N_{ad}}{\ln \sigma_w} \sqrt{\frac{\pi}{2}} r_{d0}^{4(1+\beta)/3} b^{2/3}, \quad S_w < 1, \qquad (67)$$

$$\sigma_\lambda^{ext}(S_w) = D_{2,ext}(S_w) I_{ext}(S_w), \qquad S_w \approx 1, \qquad (68)$$

$$D_{2,ext}(S_w) = \frac{N_{ad}}{\ln \sigma_w} \sqrt{\frac{\pi}{2}} r_{d0}^{2(1+\beta)} b^{2/3} \frac{b}{A_k}, \quad S_w \approx 1, \qquad (69)$$

$$I_{ext}(S_w) = \int_{r_{\min}}^{r_{\max}} \left(\frac{x}{x_{w0}}\right)^2 Q_{ext}(x, n_w) \cdot \exp\left(-\frac{1}{2} \frac{\ln^2 (x/x_{w0})}{\ln^2 \sigma_w}\right) d \ln\left(\frac{x}{x_{w0}}\right), \qquad (70)$$

where $x_{w0} = (2\pi r_{w0}/\lambda)$ is the size parameter, and r_{w0} is defined by (45), (46). For $S_w < 1$ ($s < 0$), the limits of integration $r_{\min}$ and $r_{\max}$ can be extended to 0 and ∞ with account for the fast convergence of the integrals of the lognormal spectra. For $s > 0$, $r_{\min}$ can be taken 0, and the upper limit is $r_{\max} = (2/3)(A_k/s)$. Equation (66) shows that the humidity index of extinction is $-2/3$; comparison of equations (16) and (66) with (1a), (1b) allows to relate the indices α_1 of the radius and α_2 of extinction growth factors mentioned in Introduction: there is a simple relation $\alpha_2 = 2\alpha_1$ caused by the fact that extinction by a single particle $\sim r_w^2$. Note that if to use (44) for r_{w0} in the wet lognormal spectrum instead of (45), the equations above and this relation will be somewhat more complicated.

[63] If the aerosol size spectrum is given by the inverse power law (47c), the extinction can be expressed also similar to a power law. It was shown by *Khvorostyanov and Curry* [1999b] using the similarity arguments that the humidity transformation of $Q(x_w, n_w)$ can be approximately expressed via refraction index of the dry aerosol $n_d(S_{w0})$ at some reference S_{w0}, index of pure water n_1, and of wet aerosol $n_w(S_w)$ as $Q(x, n_w) \approx Q(x, n_d)\theta(S_w)$, with the function $\theta(S_w) = (n_w(S_w) - 1)/(n_d(S_{w0}) - 1)$, where the wet index $n_w(S_w) \approx n_1 + (n_d - n_1)[(1 - S_w)/(1 - S_{w0})]$. Substituting this $Q(x, n_w)$ and spectrum (47c) into (65) and introducing notations $R = (\mu - 1)/3$, $\gamma_A = \mu - 3$ yields

$$\sigma_\lambda^{ext}(S_w) = D_{1,ext} \lambda^{-\gamma_A} \left(1 + \frac{b}{-\ln S_w}\right)^R [\theta(S_w)]^{\gamma_A} - D_{2,ext} \lambda^{-(\gamma_A+1)} \frac{bA_k}{3(-\ln S_w)^2} \cdot \left(1 + \frac{b}{-\ln S_w}\right)^{R-1} [\theta(S_w)]^{\gamma_A+1}, \qquad (71)$$

$$D_{1,ext} = c_d \pi (2\pi)^\gamma I_{1,ext}, \quad D_{2,ext} = c_d \pi (2\pi)^{\gamma+1} I_{2,ext}, \qquad (72)$$

$$I_{i,ext} = \int_{x_{\min}}^{x_{\max}} x^{-(\gamma+i)} Q_{ext}(x, n_d) dx, \qquad i = 1, 2. \qquad (73)$$

[64] Equations (71)–(73) generalize corresponding formulae from *Khvorostyanov and Curry* [1999b] with better account for the insoluble fraction and extension to the lower humidities. An interesting feature of (71) is the explicit separation of the wavelength dependence (Angstrom's inverse power law with the indices γ_A and $\gamma_A + 1$) and humidity dependence with the indices R and $R + 1$. Except for the very high $S_w > 0.97$, the major contribution into $\sigma_\lambda^{ext}(S_w)$ comes from the first term in (71), which describes σ_λ^{ext} with good accuracy. The wavelength and humidity indices are linearly related: $R = (\gamma_A + 2)/3$, this allows determination of one of these dependencies once the other is known. For $\mu = 4$, the value of $\gamma_A = 1$ and $R = 1$; for $\mu = 3.5$, the value of $\gamma_A = 0.5$ and $R = 0.83$. Note that the same wavelength dependence is valid for the aerosol optical thickness, $\tau_\lambda \sim \lambda^{-\gamma_A}$, which is an integral of σ_λ^{ext} over height, and the values of $\gamma_A \sim 0.5$–1 for τ_λ were retrieved using the satellite data over the large areas of the globe

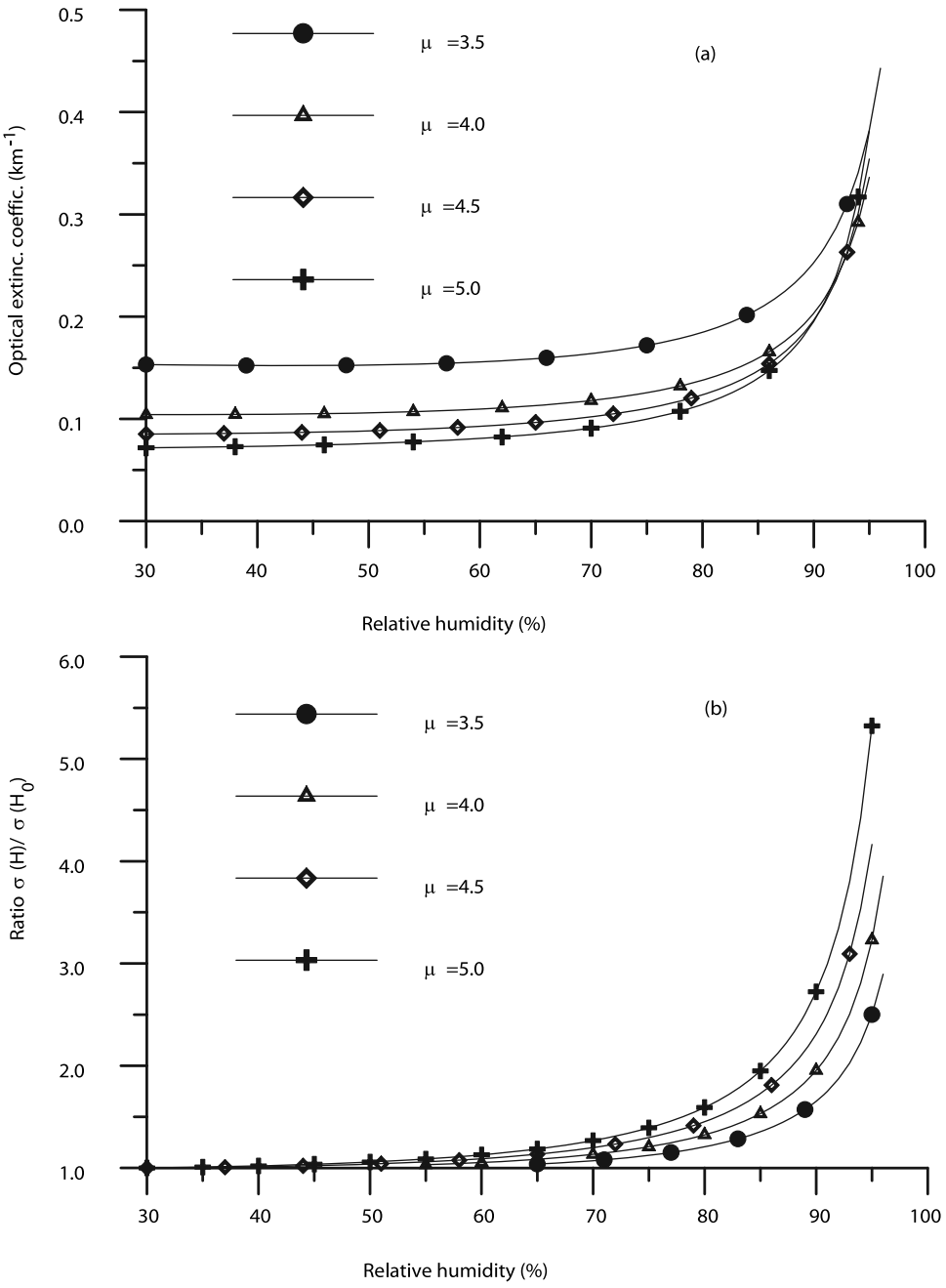

Figure 8. (a) Optical extinction coefficient $\sigma_{ext}(H)$ (km^{-1}) calculated with the wet inverse power law spectra with the indices indicated in the legend, $N_a = 10^3$ cm^{-3}, $r_{min} = 0.1$ μm (accumulation mode is accounted for), $\beta = 0.5$, and $b = 0.25$ (AP with 50% of ammonium sulfate). (b) Ratio $\sigma_{ext}(H)/\sigma_{ext}(H_0)$ with $H_0 = 30\%$.

[e.g., *Nakajima and Higurashi*, 1998]. The correction $\theta(S_w)$ due to refraction index decreases from 1 at S_{w0} to 0.65–0.7 at $S_w = 0.95$ and reduces σ_λ^{ext} by ~30–35%.

[65] *Kotchenruther et al.* [1999] found the best fit to the measured extinction as a superposition of the two empirical dependencies: $\sigma_\lambda^{ext} \sim (1 - S_w)^{-c_1}$ at high S_w and $\sigma_\lambda^{ext} \sim 1 + c_2 S_w^{c_3}$ at low S_w with c_1–c_3 being some fitting parameters. It is easy to see that (71) provides both these limits. At sufficiently high humidities and dilution, when $b/(-\ln S_w) \gg 1$ and $-\ln S_w \approx 1 - S_w$, the first major term in (71) yields $\sigma_\lambda^{ext} \sim (1 - S_w)^{-R}$. At low $S_w \sim 0.2$–0.4, so that $S_w \ll 1$, and low soluble fraction ($b/(-\ln S_w) \ll 1$), we obtain by expansion into the power series by S_w another limit, $\sigma_\lambda^{ext} \sim (1 + bR\sum_{k=0}^{n} S_w^k)$. The first limit coincides with the corresponding limit from *Kotchenruther et al.* [1999], and the second limit is an extension of that by *Kotchenruther et al.* [1999], where the series was truncated. This provides a theoretical basis for the empirical fits.

[66] Shown in Figure 8 is an example of calculations with (71) of $\sigma_\lambda^{ext}(H)$ at $\lambda = 0.5$ μm as a function of relative humidity $H = 100 \times S_w$ (as the experimental data are

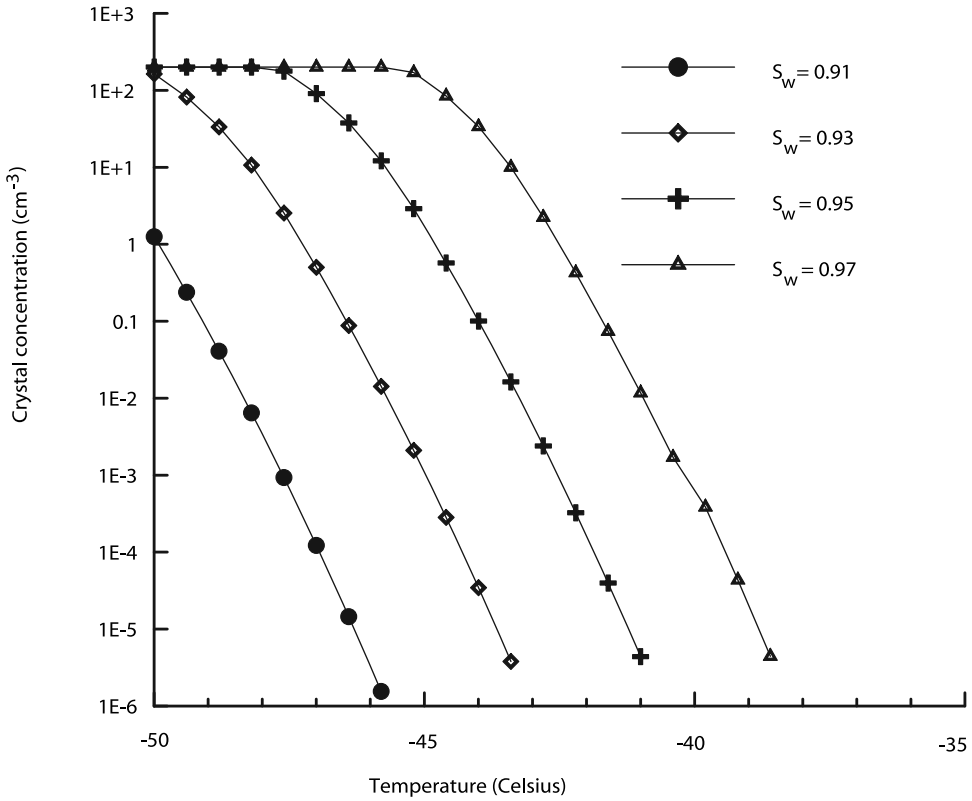

Figure 9. Concentration of the crystals homogeneously nucleated from haze particles with 50% of ammonium sulfate and wet lognormal spectrum (41) corresponding to the dry spectrum (40) with median radius $r_{d0} = 0.02$ μm, dispersion $\sigma_d = 2.5$, and concentration $N_a = 200$ cm^{-3}. The wet spectrum at each S_w is calculated with (41), (42), and (45).

usually presented) and of the extinction growth factor $\sigma_\lambda^{ext}(H)/\sigma_\lambda^{ext}(H_0)$ with $H_0 = 30\%$. Calculations are performed with 4 indices, $\mu = 3.5$ to 5, indicated in the legend, $N_a = 10^3$ cm^{-3}, $r_{\min} = 0.1$ μm, $r_{\max} = 1$ μm (only accumulation mode is accounted for, which gives the major contribution), $\beta = 0.5$, $b = 0.25$ (aerosol particles with 50% of ammonium sulfate). The values of $\sigma_\lambda^{ext}(H)$ and of the extinction *GF* are comparable to those typical measured [e.g., *Kasten*, 1969; *Fitzgerald*, 1975; *Hänel*, 1976; *Hegg et al.*, 1996; *Kotchenruther et al.*, 1999]. The extinction increases slowly at $H < 70-80\%$, and much faster after that; the *GF* reaches 1.2–1.7 at $H = 80\%$ and 3–5 at $H = 95\%$. The extinction decreases but *GF* increases with increasing μ, i.e., with increase of the spectral slope.

6.2. Ice Nucleation

[67] Ice nucleation in cirrus clouds via homogeneous freezing of haze particles usually proceeds at water subsaturation in the region $S_w \sim 0.90-0.97$ [e.g., *Sassen and Dodd*, 1988; *DeMott et al.*, 1994; *Jensen et al.*, 1994; *Heymsfield and Miloshevich*, 1995; *Khvorostyanov and Sassen*, 1998, 2002; *Sassen et al.*, 2002; *Lin et al.*, 2002; *Khvorostyanov and Curry*, 2005; *Khvorostyanov et al.*, 2006]. The wet size spectrum (32), (41) or (47c) can be also used to calculate the homogeneous ice crystal nucleation in a polydisperse haze. If the homogeneous nucleation rate is J_h, then the number of haze droplets N_i frozen in a time step Δt in a model (the number of nucleated crystals) can be calculated as (PK97)

$$N_i(\Delta t) = \int_0^\infty [1 - \exp(-V(r_w) J_h \Delta t)] f_w(r_w) dr_w, \qquad (74)$$

where $V(r_w)$ is the volume of a haze particle with radius r_w. An example of calculations of N_i was performed with (74) at various S_w. The value of J_h depends on the free energy ΔF_{cr} and critical radius r_{cr} of an ice germ and can be expressed via the temperature and water activity [e.g., *Dufour and Defay*, 1963; PK97]. Evaluation of the water activity inside each drop in a haze population can be a time-consuming process. The simpler expressions for ΔF_{cr} and r_{cr} as functions of two variables, the temperature and ambient water saturation ratio S_w, have been derived by *Khvorostyanov and Sassen* [1998, 2002], *Khvorostyanov and Curry* [2004] and were used here.

[68] The dry aerosol spectrum was lognormal (40) with median radius $r_{d0} = 0.02$ μm, dispersion $\sigma_d = 2.5$ and concentration $N_a = 200$ cm^{-3}. Such parameters for the haze consisting of sulfuric acid particles were used in the Cirrus Parcel Model Comparison Project (CPMCP), but here we considered a dry haze consisting of mixed aerosol particles with 50% of ammonium sulfate as a soluble fraction, then $b = 0.25$. According to section 4.2, the wet spectrum $f_w(r_w)$

is also lognormal (41) and r_{w0}, σ_w are calculated at each S_w with (42) and (45). Figure 9 shows that increase in S_w by 0.02 (2% of H only) causes grows in N_i by about 3 orders of magnitude, thus N_i is extremely sensitive to the evolution of the haze spectrum with variations in S_w. We performed also calculations with aerosol particles of pure sulfuric acid and the same initial lognormal spectrum as in CPMCP; for this case, $b \approx 1$ as follows from (6). The results and dependence on humidity were similar (not shown), but the concentration of nucleated crystals was higher.

[69] The effects of humidity on aerosol size spectra during ice nucleation are usually accounted for with various numerical calculations of the haze particles hygroscopic growth [e.g., *Lin et al.*, 2002], which may be rather time consuming. The use of the equations (41), (42), (46), as illustrated here, allows fast evaluation of the wet spectra and may significantly shorten calculations.

7. Conclusions

[70] Hygroscopic growth of mixed (partially soluble) aerosol particles and CCN activation are considered using a more complete version of the Köhler equation that does not assume a dilute solution and accounts for the effect of insoluble aerosol fraction. Analytical solutions to the Köhler equation are obtained for aerosol soluble fractions proportional to the volume or to the surface area of the aerosol particle. The results are briefly summarized as follows.

[71] Approximate analytical expressions for the equilibrium wet radii r_w of mixed aerosol particles and radius growth factors are derived as a function of saturation ratio at subsaturation and near saturation in cloud, which generalize the previous analogous expressions by the more detailed account for the effect of insoluble fraction and without the assumption of a dilute solution. The dilute approximation can be violated for aerosol particles with small soluble fraction at subsaturations and even at the stage of activation [*Hänel*, 1976; PK97, Table 6.2].

[72] Analytical expressions for the critical radius r_{cr} and supersaturation s_{cr} of drop activation are derived without assumption of a dilute solution. These formulae generalize the known classical equations for these quantities obtained in the high dilution approximation, allow estimation of their accuracy and areas of applicability, permit evaluation of r_{cr} and s_{cr} for the volume-proportional and surface-proportional soluble fractions and for very small soluble fractions (down to 10^{-2}–10^{-3}). The last case may be important, in particular, for evaluation of drop nucleation on the mineral dust aerosols with thin soluble coatings.

[73] The equations for the equilibrium wet radius are used to develop a simple but general method for calculation of the wet aerosol size spectra from the dry size spectra. Such methods have been developed previously for lognormal spectra and for Junge-type inverse power laws. Here this method is extended for arbitrary shape of the size spectra, analytical or measured, by considering the particles conservation law and deriving a reverse dependence of the wet radius as a function of the dry radius. A simple rule of recalculation from the dry to the wet spectra is formulated for a general case of the lognormal size spectra if the dry and wet radii are related by a nonlinear power law relation.

[74] The analytical equations for the critical radii and supersaturation are used to develop a method that allows calculation of the CCN activity spectra from arbitrary CCN size spectra, extending previous methods that have considered power law, lognormal and sectional representations of the size spectra This is also achieved by considering the particle conservation law and deriving the inverse relations $r_d(s_{cr})$ that are found as the solutions to the Köhler equation. A simple rule for recalculation from the dry spectra to the activity spectra is presented for a general case of the lognormal spectra if the dry radius and critical supersaturation are related by a nonlinear power law relation. We have extended previous parameterizations that assume volume proportional soluble fraction by introducing surface proportional soluble fractions, which may be more appropriate for insoluble particles with a soluble surface coating.

[75] **Acknowledgments.** This research has been supported by the DOE Atmospheric Radiation Measurement Program and NASA Modeling and Prediction (MAP) Program. The two anonymous reviewers are thanked for the valuable remarks that helped to improve the text. Jody Norman is thanked for help in preparing the manuscript.

References

Abdul-Razzak, H., and S. J. Ghan (2000), A parameterization of aerosol activation: 2. Multiple aerosol types, *J. Geophys. Res.*, *105*, 6837–6844.

Abdul-Razzak, H., S. J. Ghan, and C. Rivera-Carpio (1998), A parameterization of aerosol activation: 1. Single aerosol type, *J. Geophys. Res.*, *103*, 6123–6131.

Albrecht, B. (1989), Aerosols, cloud microphysics and fractional cloudiness, *Science*, *245*, 1227–1230.

Asa-Awuku, A., and A. Nenes (2007), Effect of solute dissolution kinetics on cloud droplet formation: Extended Köhler theory, *J. Geophys. Res.*, doi:10.1029/2005JD006934, in press.

Bauer, S. E., and D. Koch (2005), Impact of heterogeneous sulfate formation at mineral dust surfaces on aerosol loads and radiative forcing in the Goddard Institute for Space Studies general circulation model, *J. Geophys. Res.*, *110*, D17202, doi:10.1029/2005JD005870.

Bigg, E. K., and C. Leck (2001a), Cloud-active particles over the central Arctic Ocean, *J. Geophys. Res.*, *106*, 32,155–32,166.

Bigg, E. K., and C. Leck (2001b), Properties of the aerosol over the central Arctic Ocean, *J. Geophys. Res.*, *106*, 32,101–32,109.

Brechtel, F. J., and S. M. Kreidenweis (2000a), Predicting particle critical supersaturation from hygroscopic growth measurements in the humidified TDMA. Part I: Theory and sensitivity studies, *J. Atmos. Sci.*, *57*, 1854–1871.

Brechtel, F. J., and S. M. Kreidenweis (2000b), Predicting particle critical supersaturation from hygroscopic growth measurements in the humidified TDMA. Part II: Laboratory and ambient studies, *J. Atmos. Sci.*, *57*, 1872–1887.

Charlson, R. J., J. H. Seinfeld, A. Nenes, M. Kulmala, A. Laaksonen, and M. C. Faccini (2001), Reshaping the theory of cloud formation, *Science*, *292*, 2005–2026.

Chen, J.-P. (1994), Theory of deliquescence and modified Köhler curves, *J. Atmos. Sci.*, *51*, 3505–3516.

Chylek, P., and J. G. D. Wong (1998), Erroneous use of the modified Köhler equation in cloud and aerosol physics applications, *J. Atmos. Sci.*, *55*, 1473–1477.

Cohard, J.-M., J.-P. Pinty, and C. Bedos (1998), Extending Twomey's analytical estimate of nucleated cloud droplet concentrations from CCN spectra, *J. Atmos. Sci.*, *55*, 3348–3357.

Cohard, J.-M., J.-P. Pinty, and K. Suhre (2000), On the parameterization of activation spectra from cloud condensation nuclei microphysical properties, *J. Geophys. Res.*, *105*, 11,753–11,766.

Curry, J. A., and P. J. Webster (1999), *Thermodynamics of Atmospheres and Oceans*, 467 pp., Elsevier, New York.

Curry, J. A., et al. (2000), FIRE Arctic clouds experiment, *Bull. Am. Meteorol. Soc.*, *81*, 5–29.

Defay, R., I. Prigogine, and A. Bellemans (1966), *Surface Tension and Absorption*, 432 pp., John Wiley, Hoboken, N. J.

DeMott, P. J., M. P. Meyers, and W. R. Cotton (1994), Parameterization and impact of ice initiation processes relevant to numerical model simulation of cirrus clouds, *J. Atmos. Sci.*, *51*, 77–90.

Dick, W. D., P. Saxena, and P. H. McMurry (2000), Estimation of water uptake by organic compounds in submicron aerosols measured during the Southeastern Aerosol and Visibility Study, *J. Geophys. Res.*, *105*, 1471–1479.

Dufour, L., and R. Defay (1963), *Thermodynamics of Clouds*, 255 pp., Elsevier, New York.

Falkovich, A. H., E. Ganor, Z. Levin, P. Formenti, and Y. Rudich (2001), Chemical and mineralogical analysis of individual mineral dust particles, *J. Geophys. Res.*, *106*, 18,029–18,036.

Feingold, G., B. Stevens, W. R. Cotton, and R. L. Walko (1994), An explicit cloud microphysics/LES model designed to simulate the Twomey effect, *Atmos. Res.*, *33*, 207–233.

Fitzgerald, J. W. (1975), Approximation formulas for the equilibrium size of an aerosol particle as function of its dry size and composition and ambient relative humidity, *J. Appl. Meteorol.*, *14*, 1044–1049.

Fitzgerald, J. W., W. A. Hoppel, and M. A. Vietty (1982), The size and scattering coefficient of urban aerosol particles at Washington D.C. as a function of relative humidity, *J. Atmos. Sci.*, *39*, 1838–1852.

Fountoukis, C., and A. Nenes (2005), Continued development of a cloud droplet formation parameterization for global climate models, *J. Geophys. Res.*, *110*, D11212, doi:10.1029/2004JD005591.

Ghan, S., C. Chuang, and J. Penner (1993), A parameterization of cloud droplet nucleation. Part 1. Single aerosol species, *Atmos. Res.*, *30*, 197–222.

Ghan, S., C. Chuang, R. Easter, and J. Penner (1995), A parameterization of cloud droplet nucleation. 2. Multiple aerosol types, *Atmos. Res.*, *36*, 39–54.

Ghan, S., L. Leung, R. Easter, and H. Abdul-Razzak (1997), Prediction of cloud droplet number in a general circulation model, *J. Geophys. Res.*, *102*, 777–794.

Hämeri, K., M. Vakeva, H.-C. Hansson, and A. Laaksonen (2000), Hygroscopic growth of ultrafine ammonium sulphate aerosol measured using an ultrafine tandem differential mobility analyzer, *J. Geophys. Res.*, *105*, 22,231–22,242.

Hämeri, K., A. Laaksonen, M. Vakeva, and T. Suni (2001), Hygroscopic growth of ultrafine sodium chloride particles, *J. Geophys. Res.*, *106*, 20,749–20,757.

Hänel, G. (1976), The properties of atmospheric aerosol particles as functions of the relative humidity at thermodynamic equilibrium with the surrounding moist air, *Adv. Geophys.*, *19*, 73–188.

Hegg, D. A., D. S. Covert, M. J. Rood, and P. V. Hobbs (1996), Measurements of aerosol optical properties in marine air, *J. Geophys. Res.*, *101*, 12,893–12,903.

Heymsfield, A. J., and L. M. Miloshevich (1995), Relative humidity and temperature influences on cirrus formation and evolution: Observations from wave clouds and FIRE-II, *J. Atmos. Sci.*, *52*, 4302–4323.

Jensen, E. J., O. B. Toon, D. L. Westphal, S. Kinne, and A. J. Heymsfield (1994), Microphysical modeling of cirrus: 1. Comparison with 1986 FIRE IFO measurements, *J. Geophys. Res.*, *99*, 10,421–10,442.

Kasten, F. (1969), Visibility forecast in the phase of pre-condensation, *Tellus*, *21*(5), 631–635.

Khvorostyanov, V. I., and J. A. Curry (1999a), A simple analytical model of aerosol properties with account for hygroscopic growth: 1. Equilibrium size spectra and CCN activity spectra, *J. Geophys. Res.*, *104*, 2163–2174.

Khvorostyanov, V. I., and J. A. Curry (1999b), A simple analytical model of aerosol properties with account for hygroscopic growth: 2. Scattering and absorption coefficients, *J. Geophys. Res.*, *104*, 2175–2184.

Khvorostyanov, V. I., and J. A. Curry (2004), The theory of ice nucleation by heterogeneous freezing of deliquescent mixed CCN. Part 1: Critical radius, energy and nucleation rate, *J. Atmos. Sci.*, *61*, 2676–2691.

Khvorostyanov, V. I., and J. A. Curry (2005), The theory of ice nucleation by heterogeneous freezing of deliquescent mixed CCN. Part 2: Parcel model simulation, *J. Atmos. Sci.*, *62*, 261–285.

Khvorostyanov, V. I., and J. A. Curry (2006), Aerosol size spectra and CCN activity spectra: Reconciling the lognormal, algebraic and power laws, *J. Geophys. Res.*, *111*, D12202, doi:10.1029/2005JD006532.

Khvorostyanov, V., and K. Sassen (1998), Towards the theory of homogeneous nucleation and its parameterization for cloud models, *Geophys. Res. Lett.*, *25*, 3155–3158.

Khvorostyanov, V. I., and K. Sassen (2002), Microphysical processes in cirrus and their impact on radiation: A mesoscale modeling perspective, in *Cirrus*, edited by D. Lynch et al., 397–432, Oxford Univ. Press, New York.

Khvorostyanov, V. I., H. Morrison, J. A. Curry, D. Baumgardner, and P. Lawson (2006), High supersaturation and modes of ice nucleation in thin tropopause cirrus: Simulation of the 13 July 2002 Cirrus Regional Study of Tropical Anvils and Cirrus Layers case, *J. Geophys. Res.*, *111*, D02201, doi:10.1029/2004JD005235.

Köhler, H. (1936), The nucleus in and the growth of hygroscopic droplets, *Trans. Faraday Soc.*, *32*, 1152–1161.

Kotchenruther, R. A., P. V. Hobbs, and D. A. Hegg (1999), Humidification factors for atmospheric aerosols off the mid-Atlantic coast of the United States, *J. Geophys. Res.*, *104*, 2239–2251.

Kreidenweis, S. M., K. Koehler, P. J. DeMott, A. P. Prenni, C. Carrico, and B. Ervens (2005), Water activity and activation diameters from hygroscopicity data—Part I: Theory and application to inorganic salts, *Atmos. Chem. Phys.*, *5*, 1357–1370.

Kulmala, M., A. Laaksonen, P. Korhonen, T. Vesala, T. Ahonen, and J. C. Barrett (1993), Effect of atmospheric nitric acid vapor on cloud condensation nucleus activation, *J. Geophys. Res.*, *98*, 22,949–22,958.

Laaksonen, A., P. Korhonen, M. Kulmala, and R. J. Charlson (1998), Modification of the Köhler equation to include soluble trace gases and slightly soluble substances, *J. Atmos. Sci.*, *55*, 853–862.

Laktionov, A. G. (1972), Fraction of soluble in water substances in the particles of atmospheric aerosol, *Izv. Acad. Sci. USSR Atmos. Oceanic Phys.*, Engl. Transl., *8*, 389–395.

Leck, K., E. D. Nilsson, E. K. Bigg, and L. Bäcklin (2001), Atmospheric program on the Arctic Ocean Expedition 1996 (AOE-96): An overview of scientific goals, experimental approach, and instruments, *J. Geophys. Res.*, *106*, 32,051–32,067.

Levin, L. M., and Y. S. Sedunov (1966), A theoretical model of condensation nuclei: The mechanism of cloud formation in clouds, *J. Rech. Atmos.*, *2*(2–3), 416–424.

Levin, Z., E. Ganor, and V. Gladstein (1996), The effects of desert particles coated with sulfate on rain formation in the eastern Mediterranean, *J. Appl. Meteorol.*, *35*, 1511–1523.

Lin, R.-F., D. O. Starr, P. J. DeMott, R. Cotton, K. Sassen, E. Jensen, B. Kärcher, and X. Liu (2002), Cirrus parcel model comparison project. Phase 1: The critical components to simulate cirrus initiation explicitly, *J. Atmos. Sci.*, *59*, 2305–2329.

Low, R. D. H. (1969), A generalized equation for the solution effect in droplet growth, *J. Atmos. Sci.*, *26*, 608–612.

Mason, B. J. (1971), *The Physics of Clouds*, 2nd ed., 671 pp., Clarendon, Oxford, U. K.

Nakajima, T., and A. Higurashi (1998), A use of two-channel radiances for an aerosol characterization from space, *Geophys. Res. Lett.*, *25*, 3815–3818.

Nenes, A., and J. H. Seinfeld (2003), Parameterization of cloud droplet formation in global climate models, *J. Geophys. Res.*, *108*(D14), 4415, doi:10.1029/2002JD002911.

Pinto, J. O., J. A. Curry, and J. M. Intriery (2001), Cloud-aerosol interactions during autumn over Beaufort Sea, *J. Geophys. Res.*, *106*, 15,077–15,097.

Pruppacher, H. R., and J. D. Klett (1997), *Microphysics of Clouds and Precipitation*, 2nd ed., 954 pp., Springer, New York.

Rissler, J., A. Vestin, E. Swietlicki, G. Frisch, J. Zhou, P. Artaxo, and M. O. Andreae (2006), Size distribution and hygroscopic properties of aerosol particles from dry-season biomass burning in Amazonia, *Atmos. Chem. Physics*, *6*, 471–491.

Rissman, T. A., A. Nenes, and J. H. Seinfeld (2004), Chemical amplification (or dampening) of the Twomey effect: Conditions derived from droplet activation theory, *J. Atmos. Sci.*, *61*, 919–930.

Rosenfeld, D., Y. Rudich, and R. Lahav (2001), Desert dust suppressing precipitation: A possible desertification feedback loop, *Proc. Natl. Acad. Sci. U. S. A.*, *98*, 5975–5980.

Sassen, K., and G. C. Dodd (1988), Homogeneous nucleation rate for highly supercooled cirrus cloud droplets, *J. Atmos. Sci.*, *45*, 1357–1369.

Sassen, K., Z. Wang, V. I. Khvorostyanov, G. L. Stephens, and A. Bennedetti (2002), Cirrus cloud ice water content radar algorithm evaluation using an explicit cloud microphysical model, *J. Appl. Meteorol.*, *41*, 620–628.

Sassen, K., P. J. DeMott, J. M. Prospero, and M. R. Poellot (2003), Saharan dust storms and indirect aerosol effects on clouds: CRYSTAL-FACE results, *Geophys. Res. Lett.*, *30*(12), 1633, doi:10.1029/2003GL017371.

Sedunov, Y. S. (1974), *Physics of Drop Formation in the Atmosphere*, 234 pp., John Wiley, Hoboken, N. J.

Seinfeld, J. H., and S. N. Pandis (1998), *Atmospheric Chemistry and Physics*, 1326 pp., John Wiley, Hoboken, N. J.

Shulmann, M. L., M. L. Jacobson, R. J. Charlson, R. E. Synovec, and T. E. Young (1996), Dissolution behavior and surface tension effects of organic compounds in nucleating cloud droplets, *Geophys. Res. Lett.*, *23*, 277–280.

Smirnov, V. I. (1978), On the equilibrium sizes and size spectra of aerosol particles in a humid atmosphere, *Izv. Acad. Sci. USSR Atmos. Oceanic Phys.*, Engl. Transl., *14*, 1102–1106.

Snider, J. R., S. Guibert, J.-L. Brenguier, and J.-P. Putaud (2003), Aerosol activation in marine stratocumulus clouds: Köhler and parcel theory

closure studies, *J. Geophys. Res.*, *108*(D15), 8629, doi:10.1029/2002JD002692.

Swietlicki, E., et al. (1999), A closure study of submicrometer aerosol particle behavior, *J. Atmos. Res.*, *50*, 205–240.

Swietlicki, E., et al. (2000), Hygroscopic properties of aerosol particles in the north-eastern Atlantic during ACE-2, *Tellus, Ser. B*, *52*, 201–227.

Tang, I. N., and H. R. Munkelwitz (1994), Water activities, densities, surface and refractive indices of aqueous sulfates and sodium nitrate droplets of atmospheric importance, *J. Geophys. Res.*, *99*, 18,801–18,808.

Twomey, S. (1977), *Atmospheric Aerosols*, 302 pp., Elsevier, New York.

von der Emde, K., and U. Wacker (1993), Comments on the relationship between aerosol size spectra, equilibrium drop size spectra and CCN spectra, *Contrib. Atmos. Phys.*, *66*, 157–162.

Wurzler, S., T. G. Reisin, and Z. Levin (2000), Modification of mineral dust particles by cloud processing and subsequent effect on drop size distributions, *J. Geophys. Res.*, *105*, 4501–4512.

Young, K. C., and A. J. Warren (1992), A reexamination of the derivation of the equilibrium supersaturation curve for soluble particles, *J. Atmos. Sci.*, *49*, 1138–1143.

Zhou, J., E. Swietlicki, O. H. Berg, P. A. Aalto, K. Hämeri, E. D. Nilsson, and C. Leck (2001), Hygroscopic properties of aerosol particles over the central Arctic Ocean during summer, *J. Geophys. Res.*, *106*, 32,111–32,123.

J. A. Curry, School of Earth and Atmospheric Sciences, Georgia Institute of Technology, 311 Ferst Drive, Atlanta, GA 30332-0340, USA. (curryja@eas.gatech.edu)

V. I. Khvorostyanov, Central Aerological Observatory, Dolgoprudny 141700, Russia.